RESEARCH ARTICLE

WILEY

Characterization of seasonal groundwater origin and evolution processes in a geologically heterogeneous catchment using geophysical, isotopic and hydro-chemical techniques (Lough Gur, Ireland)

David W. O'Connell[1] 🅘 | Carlos Rocha[2] | Eve Daly[3] | Raul Carrey[4,5] |
Massimo Marchesi[6] | Mariachiara Caschetto[7] | Nienke Ansems[8] | Jean Wilson[2] |
Caoimhe Hickey[9] | Laurence W. Gill[1]

[1]Department of Civil and Environmental Engineering, Trinity College Dublin, Dublin, Ireland

[2]School of Natural Sciences, Trinity College Dublin, Dublin, Ireland

[3]Earth and Ocean Sciences, National University of Ireland, Galway, Ireland

[4]Grup MAiMA, SGR Mineralogia Aplicada, Geoquímica i Geomicrobiologia, SIMGEO UB-CSIC, Departament de Mineralogia, Petrologia i Geologia Aplicada, Facultat de Ciències de la Terra, Universitat de Barcelona, Barcelona, Spain

[5]Centres Científics i Tecnològics, Universitat de Barcelona, Barcelona, Spain

[6]IT[2]E Isotope Tracer Technologies Europe srl (MI), Milan, Italy

[7]Department of Earth and Environmental Sciences, University of Milano-Bicocca, Milan, Italy

[8]Soil Geography and Landscape Group, Wageningen University, Wageningen, Netherlands

[9]Groundwater Section, Geological Survey of Ireland, Dublin, Ireland

Correspondence
David W. O'Connell, Department of Civil and Environmental Engineering, Trinity College Dublin, College Green, Museum Building, Dublin 2, Ireland.
Email: david.oconnell@tcd.ie

Abstract

Lough Gur is a shallow groundwater fed eutrophic lake situated within a small agricultural catchment containing volcanic and karst rock features in mid-west Ireland. Seasonally active conduits linking two spring discharge locations from the lake under high flow conditions were revealed using dye tracing and a terrestrial geophysical survey, highlighting the architecture of the conduit flow path from Lough Gur to its discharge spring. A radon survey combined with a lake geophysical survey identified the locations of in-lake discharge springs and thickness of the lakebed sediments. Falling head hydraulic characterization experiments illustrated the heterogenous nature of lakebed sediments and hydrograph analysis coupled with stable isotopes of water (δ^{18}O and δ^2H) revealed significant surface water - groundwater interaction during high flow periods. Significantly, δ^{18}O and δ^2H signatures plot above the global meteoric water line and local meteoric water line indicating hydration of silicate minerals and direct isotope exchange of δ^{18}O between water and rock minerals. Groundwater δ^{18}O and δ^2H signatures during low flow periods indicate that recharge sources are influenced by enriched surface waters and precipitation while a wider range of signatures during high flow periods indicates a greater variation of sources. D-excess signatures illustrate rapid rainfall infiltration under high flow conditions, thereby demonstrating the vulnerability of the groundwater, while lake water signatures confirm widespread surface water-groundwater interaction/mixing. Hydrochemical analyses confirm both silicate weathering and carbonate dissolution as primary geochemical processes with Mg/Ca ratios suggesting greater groundwater residence time during low flow periods. Correlations between δ^{13}C$_{DIC}$ and dissolved organic carbon suggest a seasonal switch in the source of DIC to groundwaters between the oxidation of organic matter in summer and dissolution of carbonate minerals in

winter. The SI saturation index for calcite (SI_C) illustrates calcium carbonate precipitation along with CO_2 evasion to be a perennial processes. Finally, the spatial variation for nitrate isotopic signatures ($\delta^{18}O_{NO3-}$ and $\delta^{15}N_{NO3-}$) suggests a number of nitrate sources to groundwaters including soil organic nitrogen, manure and/or domestic effluent with indications of denitrification processes under low flow conditions.

KEYWORDS
D-excess, geophysics, groundwater/surface water interaction, hydrogeology, isotopes, karst, lakes, tracer test, volcanic rocks

1 | INTRODUCTION

Lakes are valuable aquatic ecosystems due to the role they play in providing significant ecosystem services such as habitats for freshwater species, sediment and nutrient retention and cycling (Kidmose et al., 2015; O'Connell et al., 2020), climate change mitigation (Raymond et al., 2013) in addition to hydrological management (Schallenberg et al., 2013). Overall lake ecosystem health and the fulfilment of its ecosystem services often rely on nutrient biogeochemical cycles dependent on the quality of water discharging to the lake ecosystem, which may be from surface water or groundwater sources (O'Connell et al., 2015). The impact on lake water quality from groundwater recharge can depend on the activities in the recharge areas (Meinikmann et al., 2015; Morgenstern et al., 2015), groundwater evolution processes and flow paths (Kidmose et al., 2015; Stoliker et al., 2016) prior to discharging to the lake, in addition to the water residence time within the lake (Hampton et al., 2019). For accurate estimations of lacustrine surface water-groundwater exchanges in complex hydrogeological systems, it is important to gain detailed knowledge on the subsurface geology, groundwater hydrochemistry and flow dynamics (Katz & Bullen, 1996; Shaw et al., 2013, 2017). Such information assists greatly in sustainable water management by providing information for the calculation of water and nutrient budgets (Lin, 2011). On the catchment scale, groundwater direction and evolution processes affecting lacustrine groundwater discharge (LGD) dynamics near lakes, depends on the position of the lake in the landscape, aquifer geological characteristics and recharge source areas and distribution (Kazmierczak et al., 2016a). Near the lake shore and lakebed, groundwater flow direction and hydrochemistry may depend on the geometry and geochemical composition of lacustrine clays and sediments (Kidmose et al., 2011, 2013). Additionally, LGD rates and flow direction can depend on the anisotropy in hydraulic conductivity and lakebed conductance (Cherkauer & Nader, 1989; Kishel & Gerla, 2002) which indirectly affect biogeochemical transformations and rates of reaction governing the hydro-chemical composition of the discharging groundwater.

For groundwater fed lakes in karst aquifer systems, understanding flow dynamics can be challenging due to geological heterogeneity related to the varying amounts of fractures and conduits in the underlying limestone (Qin et al., 2017a; Shaw et al., 2013). The hydrological connection to surface water bodies in such systems, results in

uncertainties relating to groundwater flow direction and end-members, rates of groundwater discharge to the lake, and lake water residence times (Musgrove et al., 2010).

Combined geophysical, isotopic and hydro-chemical techniques can provide useful complementary information on aquifer geology, groundwater processes and dynamics for such complex hydrogeological systems. Such a combined approach can provide accurate data for improved LGD estimations in complex hydrogeological systems and contribute towards the development of more reliable lake water budgets.

Electrical geophysical methods have been used effectively in many hydrogeological applications, e.g. aquifer characterization (Comte et al., 20122012), groundwater/surface water interactions (Nyquist et al., 2008), seawater contamination (Martorana et al., 2014), and the detection of conduits for groundwater movement through typically heterogeneous karst regions (McCormack et al., 2017). Radon is a natural tracer which has also very successfully been applied to evaluate groundwater-surface water interactions (Burnett et al., 2008) locating groundwater seepage and discharge locations (Petermann et al., 2018a) and detailed water budgets within groundwater fed lakes which is gaining increased attention (Wilson et al., 2016; Wilson & Rocha, 2016). In addition, water stable isotopes of oxygen and hydrogen can serve as natural conservative tracers in aquatic ecosystems to assess many aspects of the water cycle in lacustrine environments, including groundwater discharge rates (Krabbenhoft et al., 1990; Mitchell, 2014; Shaw et al., 2017) groundwater recharge source areas (Kamtcheung et al., 2015; Qian et al., 2014; Zhan et al., 2016) lake water residence time (Gibson et al., 2016; Petermann et al., 2018b) runoff sources to lakes and mean evaporation (Bowen et al., 2018; Cui & Li, 2015; Gibson et al., 2002) and water mixing processes (Halder et al., 2013; Jiang et al., 2018). Stable isotopes of nitrogen may also be used to establish groundwater recharge source areas and evolution processes (Yin et al., 2020). Furthermore, previous studies have shown that nitrogen cycling is tightly coupled with carbonate weathering, particularly in karst areas (Li et al., 2010a; Yue et al., 2015a).

This study was conducted in the Lough Gur catchment (Co. Limerick, Ireland), which contains a groundwater fed lake in a small agricultural catchment dominated by karst and volcanic geology. Furthermore, the study serves as an example of how complementary results from multiple analytical techniques can be applied to give more detailed information on groundwater flow and evolution in complex geological settings prior to quantitative estimations. Specifically, the study illustrates how a combined approach using geophysical, isotopic and hydro-

chemical techniques may be used to investigate: (1) seasonal dynamics of groundwater origin and flow-path networks within a geologically heterogeneous groundwater fed lake catchment; and (2) water-rock interactions and associated groundwater recharge and evolution processes.

1.1 | Study site description

Lough Gur is a popular archaeological and tourism site in County Limerick, mid-west Ireland. The lough itself is a shallow, groundwater fed, eutrophic lake (~79 ha lake surface area) with a mean depth of 1.59 m, located approximately 20 km south of Limerick City (Figure 1) The type of precipitation is predominantly rainfall with the annual average rainfall over the study period (2014–2017) is ~1026.62 mm/year. The mean average air temperature is 10.8°C and the temperature ranges on average between 18.8 and 2.3°C. The lake is surrounded and enclosed by limestone and volcanic hills, which slope steeply down to the lake's edge with a catchment elevation range of ~72–145 mOD (meters over datum). Beyond the hills, the ground slopes away to rivers and streams that are at a lower elevation than the lake itself. Therefore, Lough Gur and the surrounding hills are slightly elevated above the regional landscape (Ball, 2004). There is no perennial surface water inflow to the lake. During winter, water flows via a man-made channel into the lake from a wetland area to the southwest known as the Lake Bog which receives water from groundwater springs and the surrounding landscape. The original outflow discharges via a swallow hole called "Pollavaddra", at the north-eastern end of the lake. The sinkhole emerges at a spring (SW2) ~1800 m to the west (Figure 1). The artificial channel drains the lake during times of high-water levels and discharges to the Ballycullane River, approximately 780 m west of the north-western corner of the lake. The relatively shallow mean water depth indicates that light may penetrate the full water depth, stimulating photosynthesis and algal production, thereby impacting water quality (Layden, 1993).

Bedrock outcrop and sub-crop extend from the Grange Hill area and Knockfennell to the N-NW of the lake, in addition to Knockroe and along the eastern lake margin, including Knockadoon Hill which extends out into the lake. Within the Lough Gur catchment exists a multilayer aquifer system (Figure 2a,b), with an upper water level in volcanic bedrock to the E-NE, which is partially disconnected from a lower water table within the underlying limestone bedrock (Ball, 2004). Such a contrasting geological network makes Lough Gur an ideal location to highlight the importance of understanding the resulting hydrogeological complexity in order to gain a comprehensive conceptual model of such groundwater fed aquatic ecosystems.

2 | MATERIALS AND METHODS

2.1 | Local geology, groundwater geochemical tracing, geophysical survey

Information on the local geology of the Lough Gur catchment was gathered from geological map datasets of the Geological Survey of

Ireland and Limerick county council as well as information from academic literature (Ball, 2004; Deakin et al., 1998; Somerville et al., 1992). Groundwater geochemical tracing was performed using continuous measurements of lake water radon activity (^{222}Rn) to qualitatively assess groundwater inputs into the lake. During a survey carried out in April 2015, lake water radon activity was continuously measured in dissolved gas in the water column from a moving vessel using two Durridge Radon-in-air monitors combined with two Liqui-Cel MiniModules® (Wilson & Rocha, 2012). Precise lake location and water depth was recorded through the concurrent use of a GPSMAP 750 s Sounder (GARMIN) and a CTD probe (Schlumberger Water Services) positioned just above the pumps (Wilson & Rocha, 2012).

A geophysical survey using Electrical Resistivity Tomography (ERT) was employed to image possible subsurface groundwater flow paths in the epikarst and upper karst network. The ERT comprised of two terrestrial transects to establish the direction and architecture of suspected karst conduits underneath Knockfennell connecting the sinkhole to discharge springs. The terrestrial ERT profiles were acquired with a 10 channel IRIS Syscal Pro resistivity meter coupled to a 48-electrode multicore cable using a standard 2D approach (Dahlin & Zhou, 2004) employing the Wenner-Schlumberger array configuration. The electrode array allowed depths of investigation of >50 m below ground level. The voltage used in the current dipole was automatically managed by the system with a maximum voltage of 800 V, and an injected current up to 0.5 A. The aquatic ERT profiles were carried out to detect suspected lakebed springs discharging groundwater into the lake with the locations based on prior Rn surveys (April 2015 and July 2017) and investigate the depth to the bedrock beneath the lakebed deposits. These ERT profiles were recorded with a boat-mounted resistivity meter connected to a surface-towed multi-core cable incorporating 13 graphite electrodes at 5 m separation survey speeds, typically ~3 km h^{-1}. The meter was coupled to an echo sounder, outputting a continuous record of the water depth, with a Trimble GPS with a positional accuracy of ±3 m. All ERT data have been inverted with Res2dinv (Geotomo Software, 2010) using a finite element forward model (Coggon, 1971) using a robust L$_1$-norm least squares Occam inversion algorithm (Claerbout and Muir, 1973) to output subsurface resistivity profiles. The least-squares approach minimized the absolute difference between the observed and calculated apparent resistivities, typically within seven iterations.

2.2 | Local hydrogeology, lake stage and surface water drainage networks

A summary of the fieldwork and timing during 2014–2017 is listed in Table S1. Water tracing experiments using fluorescent dye were undertaken to establish and confirm the connection and travel time between the swallow hole outflow (SW-4), which flows under Knockfennell hill and emerges at springs (SW-2 and SW-3) northwest of Lough Gur (Figure S1). Fluorescein dye was used under low flow (September 2014) and high flow conditions (February 2017) to carry out qualitative tracing analysis. Spring outflow locations were monitored both manually using
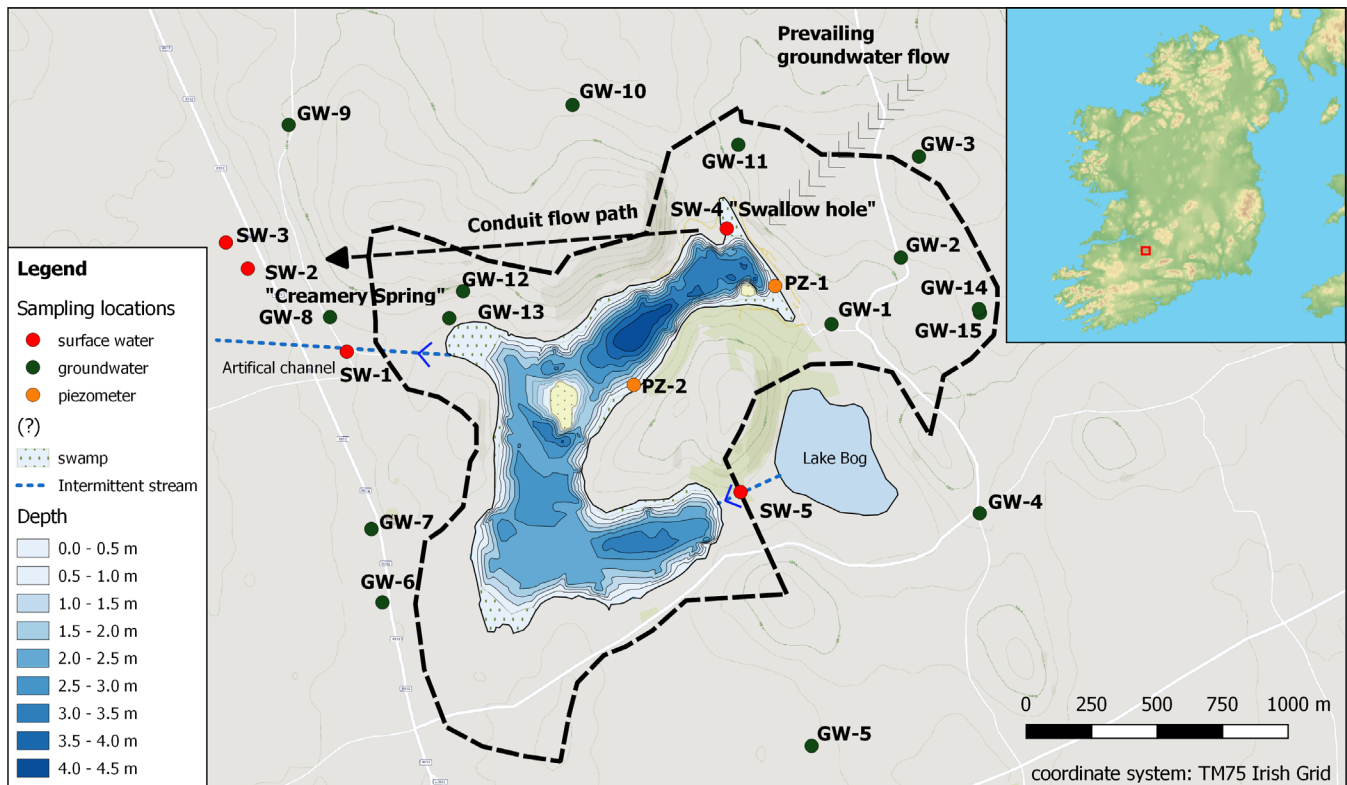
FIGURE 1 Lough Gur catchment map including the piezometer nest locations (PZ-1 and PZ-2), local household wells and boreholes (SW) including surface hydrometric and sampling stations at the lake bog inflow (SW-22), the artificial outflow channel (SW-1), the creamery well spring (SW-2), the field spring (SW-3) and the sinkhole outflow location (SW-4).

dark 100 ml bottles (September 2014) and automatically using a GGUN-FL30© flow through spectro-fluorometer (February 2017) over a period of 2 weeks. The manual samples were analysed using a Perkin Elmer LS 55 spectro-fluorometer (Hickey, 2010).

Fluctuations in lake stage were recorded over the study period using high-resolution water level loggers (Solinst© and Van Walt©) with values periodically calibrated using manual measurements. Local household wells and boreholes were surveyed and water levels measured in June 2015, July 2015, March 2016 and July 2016 (Figure 1 and Table S1). For groundwater flow patterns, hydraulic head data during the study period was utilized from measurements taken during low flow and high flow periods (O'Connell, 2015). Near-shore groundwater flow was monitored at two previously identified groundwater discharge locations in the lake by installing piezometer nests, each with three piezometers installed at approx. 1.0, 1.5 and 1.7 m depth at the amenity centre site (PZ-1) and 0.5, 1.0 and 1.5 m just offshore of Knockadoon hill (PZ-2) (Figure 1). The piezometers were made from 10 mm-internal diameter high density polyethylene (HDPE) tubing with a drive-point on one end (Rivett et al., 2008). Falling head hydraulic conductivity measurements were carried out on each of the three piezometers in the nest at the visitor centre site near the north east shore of Lough Gur (Luttenegger & DeGroot, 1992). Results were plotted with change in hydraulic head against time and analysed using the Hvorslev method (Schwartz & Zhang, 2003).

2.3 | Sampling and analysis methods

A total of 48 water samples in total (including groundwater, surface water and piezometers) were collected from various locations within the Lough Gur catchment during March 2016 and July 2016 (Figure 1), including water samples from piezometer nests and bottom waters at the amenity centre site (PZ-1) and just offshore of Knockadoon in Lough Gur (PZ-2) during the same periods. Additionally, water samples were taken from boreholes and wells using balers (biobaler©) and submersible pumps (wasp©) and from surface water including the discharge springs from the lake.

In-situ field parameters measured included pH, electrical conductivity, and temperature using a multiparameter probe (Hanna Instruments©). Samples were collected using 60 ml plastic syringes and filtered through 0.2 μm nylon filters in the field. They were stored in a cooler box and taken back to a refrigerator for storage at 2°C each day. All samples were analysed at the Environmental Engineering Research Lab and Centre for the Environment at Trinity College Dublin (TCD). Cations were analysed using a Perkin Elmer ICP-OES. Prior to analysis, the solution was acidified with 1% (vol/vol) nitric acid. Anions were analysed using ion chromatography (IC) Dionex ICS-1100. Bicarbonate was analysed almost immediately after taking the samples using the gran titration method (Stumm & Morgan, 1981). Dissolved organic carbon (DOC) were determined on a Shimadzu TOC analyser. The calcite and dolomite saturation index of all water samples were calculated by PHREEQC program. δ^2H and $\delta^{18}O$
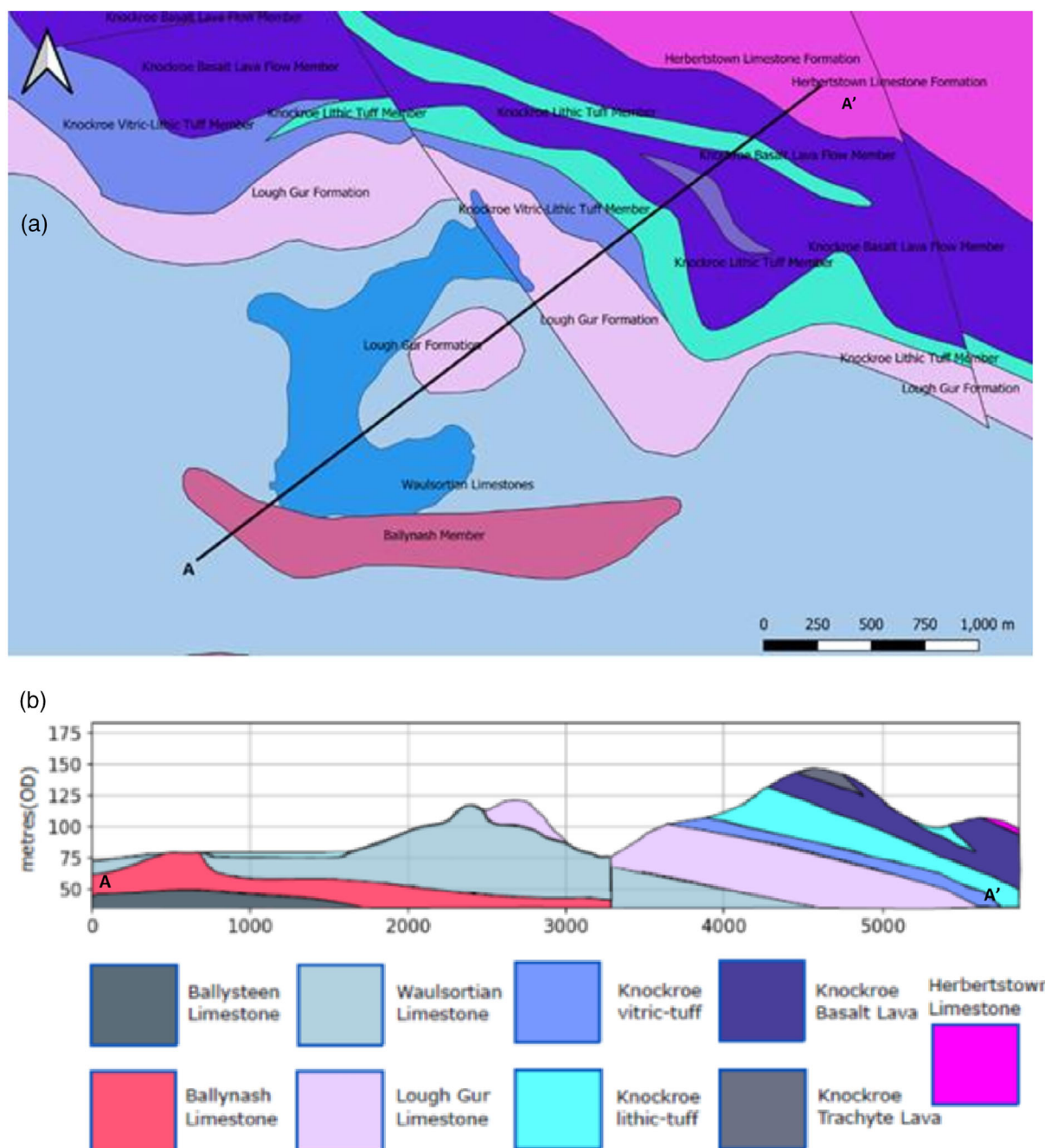
FIGURE 2 (a) Geological map of lough Gur area and (b) geological profile for section a on geological map illustrating the location of lough Gur and position of fault between Knockroe and Knockadoon. (*Source*: Modified from Ball, 2004).

isotope compositions were measured by DI-IRMS on a Delta S Finnigan Mat at the University of Barcelona using the H_2 and CO_2 equilibrium techniques respectively. The $\delta^{15}N_{NO3-}$ and $\delta^{18}O_{NO3-}$ compositions were determined following the cadmium and azide reduction methods (McIlvin & Altabet, 2005). The isotopic composition was analysed using a Pre-Con (Thermo Scientific) coupled to an IRMS (Finnigan MAT 253, Thermo Scientific). $\delta^{13}C_{DIC}$ was determined in a GasBench II (Thermo Scientific) coupled to a MAT-253 IRMS (Thermo Scientific). Notation is expressed in terms of δ (‰) relative to the international standards: Atmospheric N_2 (Air) for $\delta^{15}N$, Vienna Standard Mean Oceanic

Water (V-SMOW) for $\delta^{18}O$ and VPDB for $\delta^{13}C_{DIC}$. Following (Coplen, 2011) several international and laboratory [University of Barcelona (UB)] standards were interspersed among samples for normalization of the results. The reproducibility (1σ) of the samples, calculated from the standards systematically interspersed in the analytical batches, was ±1.0‰ for $\delta^{15}N_{NO3-}$, ±1.5‰ for $\delta^{18}O_{NO3-}$ and ±0.2‰ for $\delta^{13}C_{DIC}$. Chemical and isotopic analyses were prepared at the laboratory of the MAiMA-UB research group and analysed at the Centres Científics i Tecnològics of the Universitat de Barcelona (CCiT-UB). Isotope ratios are reported using delta (δ) expressed in per mil (‰) as follows,

$$\delta(‰) = \left(\left[R_{sample}/R_{standard} \right] - 1 \right) \times 1000 \quad (1)$$

3 | RESULTS AND DISCUSSION

3.1 | Local bedrock geology, hydrogeology and geophysical surveys

The Ballynash Member of the Ballysteen Formation is the oldest bedrock outcrop specific to the Lough Gur catchment. This unit subcrops as a "whaleback shape" along the axis of an anticline trending approximately E-W near the southern lake shoreline (Ball, 2004). The majority of the local groundwater catchment is underlain by karstic Waulsortian limestone which is one of the most extensive formations in south-western Ireland (Hitzman et al., 2002; McCusker & Reed, 2013; Murray, 2018). The higher elevation regions are underlain by the younger, Lough Gur limestone and Knockroe volcanic formation (which contain variable volcanics and are the youngest sub-crop in the catchment Ball, 2004) Figure 2b.

The two terrestrial ERT survey transects (T1 and T2) were 480 m long and run in a SE-NW direction from the northern margin of the lake (Figure 3a,b). These ERT survey transects illustrated typical resistivity values found in similar limestone formations in Ireland (McCormack et al., 2017). Bedrock resistivity values of 100–1000 Ωm at these cross sections of Knockfennell indicate the presence of epikarst with resistivities above 1000 Ωm indicative of more competent bedrock (McCormack et al., 2017). Resistivity values are lower (~700 Ωm) in general along ERT transect 1 than ERT transect 2 (2000 Ωm) which is located close to Grange Hill. The contact between the highly karstified Waulsortian limestone (GSI, 2000) and the Lough Gur limestone is visible at ~180 m along the ERT transect 1 (Figure 3a) and 310 m along ERT transect 2 (Figure 3b). To the south of this contact the resistivities range between 50 and 300 Ωm. Along ERT transect 1 there is a significantly low resistivity anomaly of ~15 Ωm at a depth of 10 m and thickness of 20 m visible within this zone at 160 m along the profile which indicate a potential water saturate zone or karst conduit. Two similar low resistivity anomalies are observed at 160 and 320 m along ERT transect 2. The low resistivity area at 320 m is likely a perched water saturated zone on
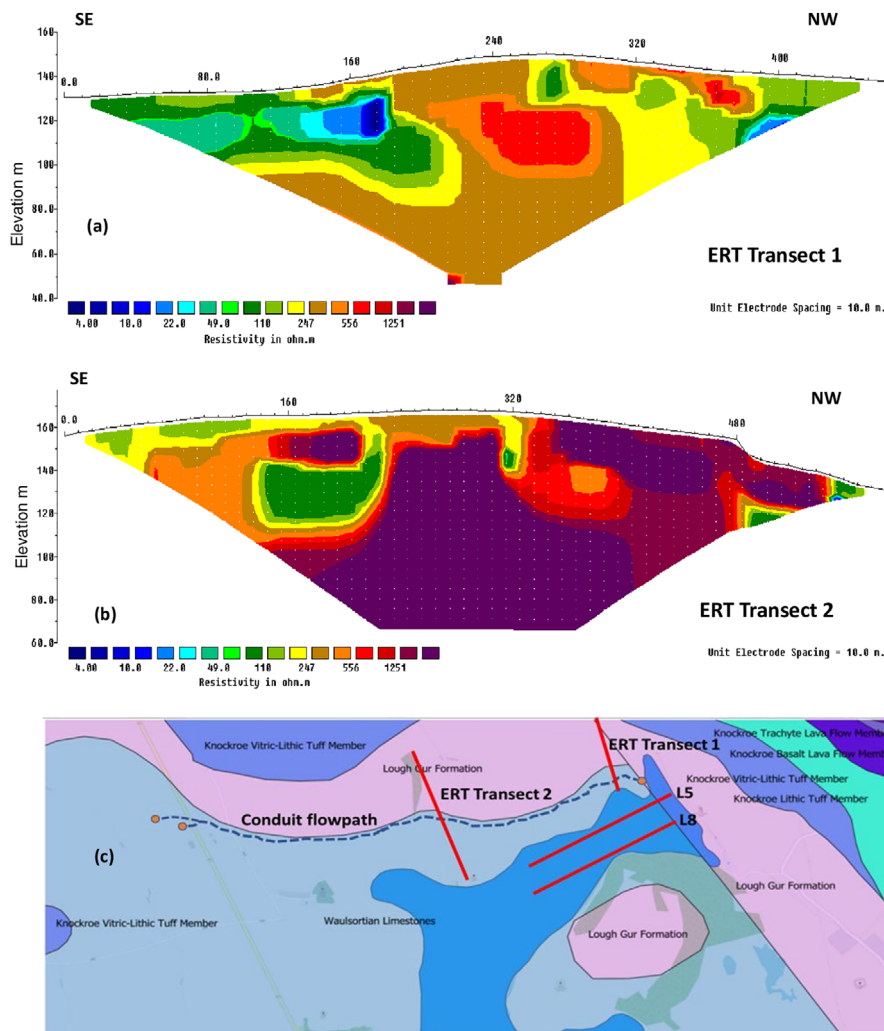

FIGURE 3 (a) ERT profile on transect 1 (~50 m long) was carried out to intersect the karst conduit groundwater flowpath approximately 30 m from the Pollavadra swallow hole (SW-4); (b) ERT profile on transect 2 (~100 m long) intersects the conduit flowpath approximately midway between the swallow hole and discharge springs at SW-2 (creamery spring) and SW-3 (field spring) and; (c) illustrates a satellite map of the locations of the ERT terrestrial (transect 1 and 2) and aquatic transects (L5 and L8) along with a tentative karst conduit groundwater flow-path (broken blue line) to the main discharge spring SW-2 (creamery spring) and the seasonally connected discharge spring SW-3 (field spring).
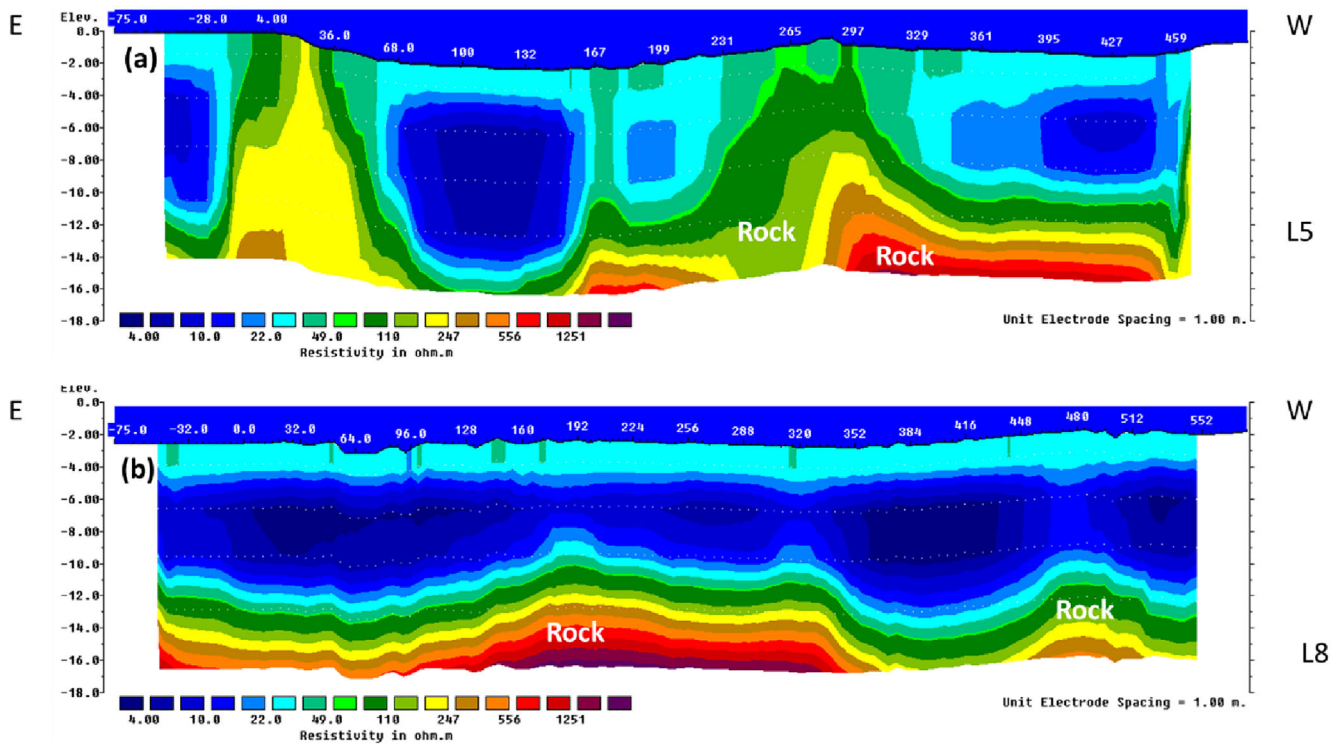
FIGURE 4 Surface-towed marine ERT profiles on lough Gur for (a) L5 and (b) L8 with estimated base of unconsolidated sediments and (≤10 Ωm) more consolidated material (≥10 Ωm).

Knockfennell (Figure 3b). The low resistivity area at 160 m along ERT transect 2 may be a continuation of the observed low resistivity area at 160 m on ERT transect 1. The locations of these low resistivity areas coupled with the geologically reflective resistivity's of the surround geology suggest this is the location of the subsurface conduit flow pathway along the interface of the Waulsortian limestone and Lough Gur limestone formations (Figure 3c), linking the sinkhole outflow at the lake with the discharge spring (SW-2) located 1.8 km down gradient to the northwest of Knockfennell. Both aquatic ERT profiles, L5 (Figure 4a) and L8 (Figure 4b) show lake water depth of approx. 1–2 m and a water resistivity of 10 Ωm. Sub-bottom resistivity's of 10–30 Ωm with a thickness of ∼10 m of sediment is visible which are thought to be predominantly low permeability clay and marl with possibly more localized areas of silts and sands. Beneath this low permeability layer, resistivity values increase indicating the karstified Waulsortian limestone underlying the lake.

3.2 | Hydrological networks and surface water – Groundwater interactions

Previously a fluorescein dye tracing experiment was carried out at the Lough Gur swallow-hole "Pollavaddra" (SW-4) (Figure S1) under low flow conditions (September 2014) which confirmed the existence of a conduit flow pathway that discharges to a spring outflow SW-2 at an old creamery location (Langford & Gill, 2016). In this study, a fluorescein dye tracing experiment was carried out under high flow

conditions (February 2017), which indicated water from the Lough Gur swallow-hole outflow (SW-4) discharged at both the creamery spring outflow (SW-2) and a field spring (SW-3) approximately 150 m to the north of the creamery spring. This result suggests that under high flow conditions the karst conduits at higher elevations in the subsurface become active and join both the creamery spring (SW-2) and the field spring (SW-3) (Figure S1).

Radon-222 surveying can be used to identify hotspots of groundwater upwelling in a cost-effective way within water bodies (Wilson & Rocha, 2012). High Radon-222, low temperature and low electrical conductivity anomalies are indicative of groundwater upwelling to the surface water body. The radon survey located three primary areas of groundwater upwelling within the lake at the amenity site along the north-eastern shore, to the north of Knockadoon and an expansive area along the northern shore of the lake (Figure 5). Groundwater levels within the Lough Gur and Waulsortian limestone are very responsive to precipitation events with short lag-times. This is illustrated for Lough Gur in the hydrographs (Figure 6) which suggests a rapid response to recharge events and is a characteristic of fissured limestone (Kovačič & Ravbar, 2010).

3.3 | Lakebed hydraulic conductivity, vertical hydraulic gradient and groundwater flux

Piezometer nests were installed into the lakebed at the amenity centre (PZ-1) and north of Knockadoon (PZ-2) which provided
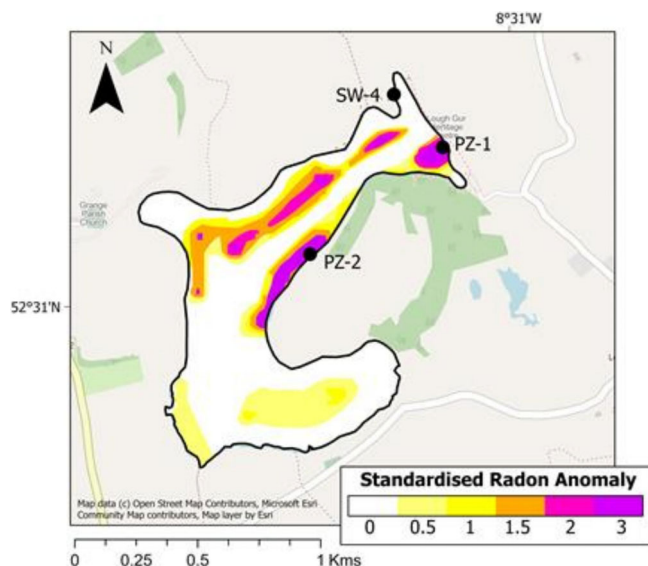
FIGURE 5 Spatial distribution of radon activity within lough Gur (April 2015) showing eastern (PZ-1) piezometer locations and northern locations (PZ-2) as radon "hotspot" location. SW-4 is the lake sinkhole "Pollavoddra"

information on lake-bed hydraulic conductivity (K_h), vertical hydraulic gradient (VHG%) and derived groundwater fluxes Table 1. Radon surveys carried out in April 2015 and July 2016 guided the installation locations of both piezometer nests. Falling head hydraulic conductivity measurements were carried out on each of the three piezometers which make up the piezometer nest at (PZ-1) near the north-east shore and at (PZ-2). For PZ-1, all mini-drive point piezometers were responsive with K_H values increasing down the sediment profile (1–1.7 m). In contrast, the K_h values at PZ-2 were more heterogenous and increase with depth in the sediment profile from the upper (1 m) to middle horizon (1.6 m) and then increase again at the deepest horizon (1.8 m) (Table 1). Although the values only represent two lake bed locations ($\sim$3 m off shore), the hydraulic conductivities are of the same general magnitude from both locations and align with typical near shore lake sediments even with some heterogeneity in hydraulic conductivity (Kazmierczak et al., 2016b; Rudnick et al., 2015).

The VHG derived groundwater discharge fluxes suggest some spatial and temporal variation in groundwater discharge to the lake Table 1 (Käser et al., 2009). The average groundwater discharge fluxes at the amenity site piezometer location show values two orders of magnitude lower at the upper sediment horizon PZ-1a (0.04 m^{-3} m^{-2} d^{-1}) in comparison to both the lower PZ-1b and PZ-1c. Notably, groundwater discharge fluxes at PZ-2 are an order of magnitude higher at the upper sediment horizon PZ-2a (0.46 m^{-3} m^{-2} d^{-1}). While there are contrasting nearshore groundwater seepage rates (m^3 m^{-2} d^{-1}) at Lough Gur for the upper PZ-1a (0.04 m^{-3} m^{-2} d^{-1}) and PZ-2a (0.46 m^{-3} m^{-2} d^{-1}) locations, these values are comparable with nearshore groundwater discharge rate heterogeneity in other groundwater fed lakes (Fellows & Brezonik, 1980; Meinikmann et al., 2015; Oliveira Ommen et al., 2012).

3.4 | Seasonal dynamics in hydrological flow-path networks

Oxygen ($\delta^{18}O$) and hydrogen (δ^2H) stable isotope signatures from groundwater are related to recharge sources, flow paths and residence times (Chen et al., 2018; Dar et al., 2021). Water isotope results for all groundwater, surface water and springs under both hydroperiods are displayed in (Figure 7a,b). All water compartments generally show distinct seasonal dynamics where there is more overlap of $\delta^{18}O$ and δ^2H stable isotope signatures under high flow conditions (Figure 7a) suggesting extensive groundwater/surface water interaction (Doctor Jr. et al., 2006; Qin et al., 2017b). Groundwater samples perennially plot above both the global meteoric water line (GMWL) and local meteoric water line (LMWL) and are relatively depleted by comparison to surface water, piezometer and bottom water samples. This is likely caused by increased fractionation in low temperature environments, due to heterogeneous geochemical reactions, which can result in $\delta^{18}O$ and δ^2H plotting above the meteoric water line (Clark & Fritz, 1997). Specifically, minerals forming metamorphic, igneous (basalts) rocks and limestones can enrich $\delta^{18}O$ and δ^2H signatures (Allegre, 2008). Such enrichment is thought to result from the hydration of silicate minerals (Brkić et al., 2016) or by direct isotope exchange of $\delta^{18}O$ between water and the mineral crystal lattice during contact with flowing groundwater in fractures and faults (Clark & Fritz, 1997). Results suggest mineral dissolution is dominant with hydration and isotope exchange reactions discriminating in favour of heavier isotopes in groundwater. These observations suggest that weathering is more rapid than mineral formation in the Lough Gur catchment, which potentially is accelerated by the CO_2 content of soils upon water infiltration.

Surface water samples are in general more enriched than groundwaters and plot below or along the GMWL or LMWL (Figure 7a,b). Surface water samples taken at the lake sinkhole (SW-4) and a groundwater borehole near the north-eastern shore of the lake (GW-1) show depleted water isotope signatures similar to groundwater under high flow conditions which indicates surface water groundwater interaction. Under low flow conditions there is distinctly more evaporative enrichment of $\delta^{18}O$ signatures for surface waters and piezometer samples than under high flow (Figure 7b). Under high flow conditions more surface water and piezometer samples plot along the GMWL and LMWL line, suggesting less evaporative enrichment, while under low flow conditions more of these samples plot below the GMWL and LMWL line confirming the impact of evaporation during periods of elevated temperatures. During the high flow recharge period the range of $\delta^{18}O$ and δ^2H values in the shallow and deep groundwater sampling boreholes and wells showed similar order of magnitudes suggesting similar climatic sources of precipitation and recharge (Huang & Wang, 2018; Murgulet et al., 2016). Seasonal variation in climatic conditions and sources of precipitation during recharge is indicated by differences in the range of $\delta^{18}O$ and δ^2H signatures of groundwaters (Marfia et al., 2004). Clustered depleted $\delta^{18}O$ values (-6.8 to -7.9 [‰]) for groundwater samples under low flow conditions suggests a recharge source influenced by slightly more enriched surface water sources in comparison to the

FIGURE 6 Hydrographs showing precipitation and surface water/ groundwater levels for GW-1, GW-13 and SW-4 (Lake water level at sinkhole) from February 2014 to May 2017.
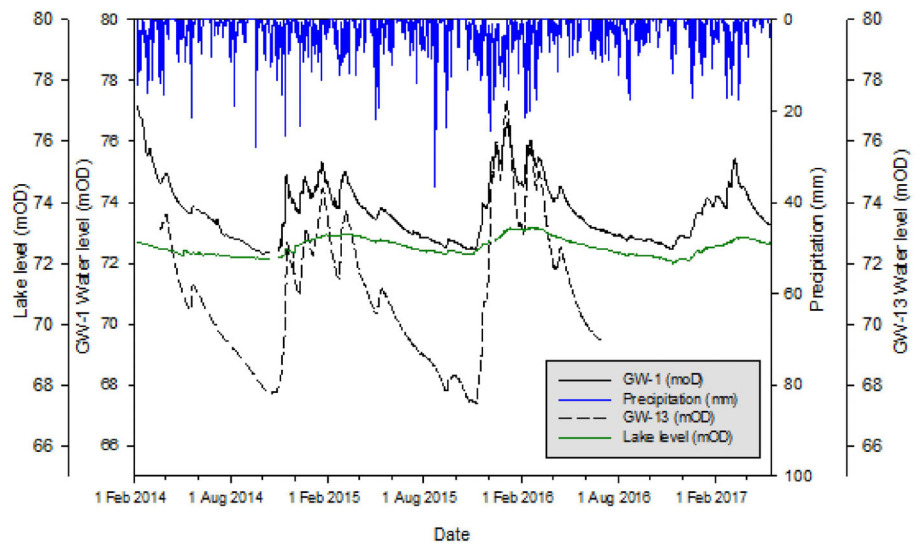

TABLE 1 Characteristics for piezometer nest one (PZ-1a, PZ-1b and PZ-1c) two at three different depths (PZ-2a, PZ-2b and PZ-2c) showing the screen depth (m), hydraulic conductivity K_h (m d^{-1}), VHG (%) and potential discharge (m^{-3} m^{-2} d^{-1}).

Piezometer	Piezometer screen depth (m)	K_h (m d^{-1})	VHG (%)	Potential discharge (m^{-3} m^{-2} d^{-1})
Piezometer 1 (PZ-1)				
PZ-1a	0.97–1.07	0.02	1.14	0.04
PZ-1b	1.43–1.53	0.09	0.78	2.18
PZ-1c	1.6–1.7	0.17	0.7	5.08
Piezometer 1 (PZ-2)				
PZ-2a	1.0–1.10	0.1	1.34	0.46
PZ-2b	1.66–1.76	0.03	1.52	0.14
PZ-2c	1.71–1.81	0.12	2.48	0.94

wide variation in recharge sources during high flow conditions suggested by the slightly wider range of δ^{18}O values (−6.9 to −9.3 [‰]), possibly due to the activation of karst conduits originally within the unsaturated zone.

The seasonal connection between the two springs to the northwest of Lough Gur, confirmed by dye tracing under high flow conditions, was further validated by the similar δ^{18}O and δ^2H stable isotope signatures of the discharging spring waters: SW-2 (−5.6, −34.6 [‰]) and SW-3 (−5.4, −34.8 [‰]). In addition, under high flow conditions the enrichment of the isotopic signatures between the lake sinkhole outflow (SW-4) (−6.5, −39.8 [‰]) and the discharge springs SW-2 (−5.6, −34.6 [‰]) and SW-3 (−5.4, −34.8 [‰]) suggests an influence from rapidly infiltrating surface waters along the karst conduit flow-path from the lake to the discharge springs (Clark & Fritz, 1997; Gil-Márquez et al., 2019; Guo et al., 2019). Further evidence is provided by the intersection of the GMWL and the local evaporation line (LEL) falling at approximately the same δ^{18}O and δ^2H stable isotope signature location of the discharging springs waters SW-2 (−5.6, −34.6 [‰]) and SW-3 (−5.4, −34.8 [‰]) which approximates for regional mean annual precipitation (Gibson et al., 2017; Tondu et al., 2013). Such infiltrating rainwater under high flow conditions has been shown

to enrich water discharging at karst springs (Guo et al., 2019). In contrast, under low flow conditions the difference in the water isotopic signatures at the discharge springs SW-2 (−5.3, −32.9 [‰]) and SW-3 (−6.0, −37.0 [‰]) validates the previous dye tracing results, suggesting a different mix of water sources to the springs under low flow conditions with SW-2 having a direct connection to the lake (Figure 7c,d).

3.5 | Water sources and mixing processes

Deuterium excess (d-excess ‰) indicates secondary processes that affect atmospheric vapour content in the evaporation-condensation cycle (Gat & Matsui, 1991; Merlivat & Jouzel, 1979). Many natural parameters affect the d-excess value of precipitation which includes air temperature and relative humidity during evaporation. The d-excess values of surface, groundwater and piezometer/lake bottom waters in Lough Gur allow the possibility of characterizing the interaction of different air masses and temporal evolution of this interaction (Yang et al., 2011). In this study, there are changes in the d-excess ranges for all water compartments under high and low flow
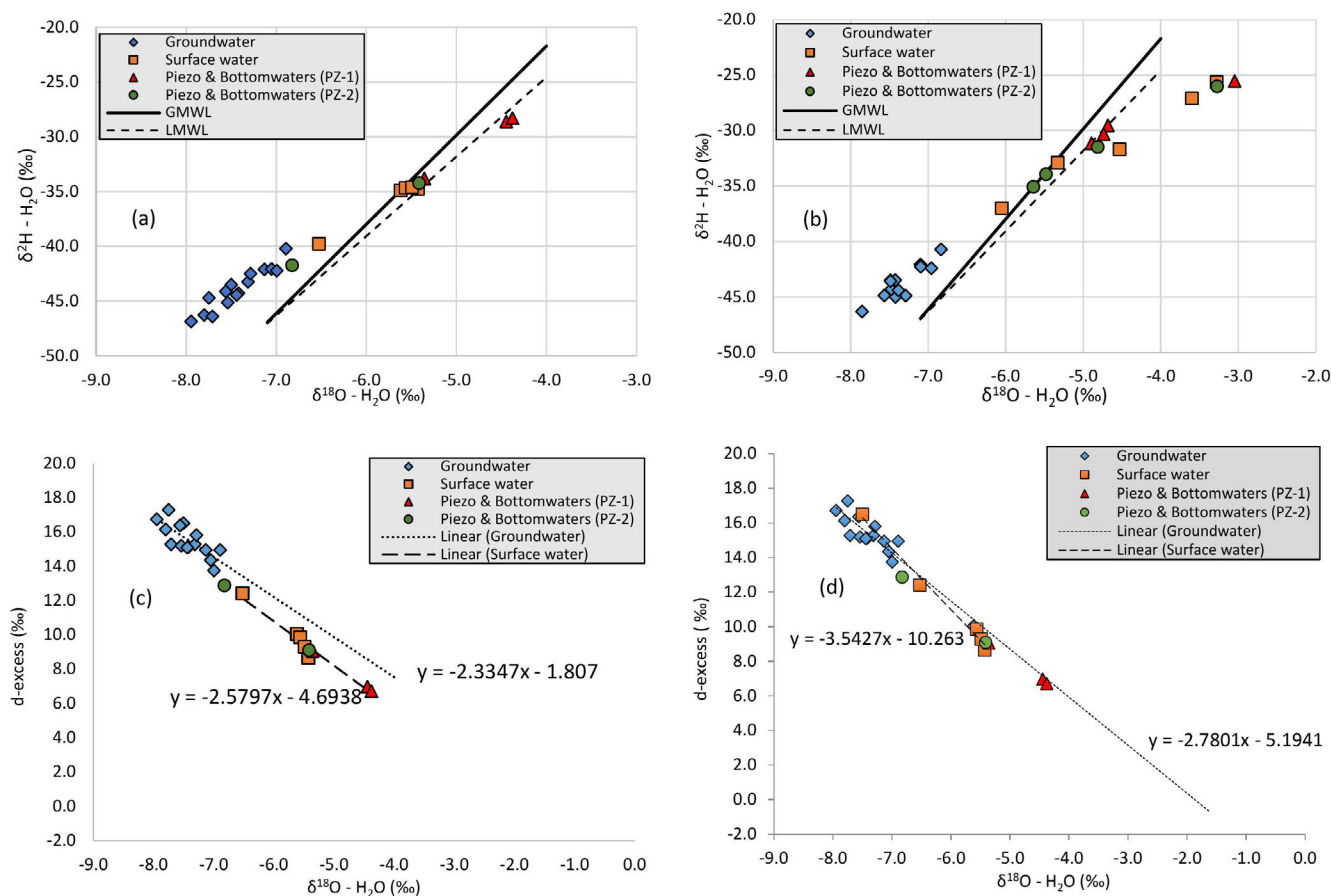
FIGURE 7 (a) High flow period (March 2016) and (b) low flow period (July 2016) deuterium (δ^2H) versus Oxygen-18 (δ^{18}O) signatures (‰) (c) high flow "period (March 2016) and (d) low flow period (July 2016) deuterium excess (d-excess) versus Oxygen-18 (δ^{18}O) signatures (‰).

conditions, as shown on Table 2 and Figure 7c,d, which can give indirect information on the seasonality of groundwater sources and flow pathways (Jasechko et al., 2014) and groundwater-surface water connectivity even in complex environmental settings (Rocha et al., 2016). The d-excess values are related to conditions of atmospheric humidity during vapour forming processes which can fluctuate seasonally due to changes in the humidity in the moisture source areas (Johnsen et al., 1989; Merlivat & Jouzel, 1979). Higher d-excess values in particular for groundwaters during high flow likely arises from rapid infiltration of precipitation associated with gulf stream sources (Marfia et al., 2004). During vapour recycling, the d-excess increases due to greater evaporate content and when water is lost through evaporation, the d-excess will decrease (Diefendorf & Patterson, 2005). Generally lower and seasonally dynamic d-excess values were identified for the surface waters and some springs in the Lough Gur catchment suggesting a significant evaporative influence (Table 2).

Under high flow conditions the SW-1 (artificial channel) outflow shows similar d-excess values to groundwater from the eastern side of the lake and groundwater in proximity to the artificial channel (Figure 7c) which indicates a widespread contribution or mixing of groundwater sources to the lake and springs. In addition,

the lower d-excess values indicate some evaporation of water in the lake bog fen area (Ala-aho et al., 2018). In contrast, during low flow conditions (Figure 7d), the SW-3 (field spring) and SW-2 (creamery spring) show a more distinct signal which suggests different sources during the low flow periods, confirming dye tracing results. The lower d-excess value of SW-2 (creamery spring) illustrates the greater evaporative influence from lake water in comparison to the higher d-excess values of SW-3 (field spring) indicative of more rapid infiltration with less evaporative losses (Gautam et al., 2018). Similar d-excess values exist between SW-4 (sinkhole) and the bottom-waters at the PZ-2 piezometer nest suggesting efficient lake water mixing with a similar evaporative influence (Shaw et al., 2017).

3.6 | Groundwater recharge and geochemical indicators

The geological sources and controlling processes of groundwater recharge and evolution within the catchment may be investigated using bivariate analyses of ionic relations (Zhu et al., 2011). In this regard, molar bivariate plots were made of Na-normalized Ca, Mg and

TABLE 2 D-excess values under high flow (March 2016) and low flow (July 2016) conditions for surface waters, ground-waters and piezometer nests in the lough Gur catchment.

March 2016 (high flow)	δ^2H excess, d (‰)	July 2016 (low flow)	δ^2H excess, d (‰)
Surface water			
SW-1 (artificial channel)	16.50	SW-1 (artificial channel)	1.72
SW-2 (creamery well)	9.86	SW-2 (creamery well)	9.75
SW-3 (field well)	8.66	SW-3 (field well)	11.37
SW-4 (sinkhole)	12.41	SW-4 (sinkhole)	0.63
SW-5 (flow from bog)	9.30	SW-5 (flow from bog)	4.55
Groundwater			
GW-1	10.05	GW-1	14.74
GW-2	14.95	GW-2	15.65
GW-3	16.37	GW-3	14.49
GW-4	16.73	GW-4	—
GW-5	15.11	GW-5	16.50
GW-6	14.35	GW-6	13.45
GW-7	16.14	GW-7	14.36
GW-8	15.28	GW-8	—
GW-9	15.19	GW-9	—
GW-10	15.28	GW-10	13.96
GW-11	14.94	GW-11	16.37
GW-12	15.80	GW-12	13.27
GW-13	13.75	GW-13	15.50
GW-14 (Depth - 11.71)	15.09	GW-14 (Depth- 11.71)	15.92
GW-15 (Depth - 26.02)	17.29	GW-15 (Depth- 26.02)	16.32
Piezometer (AC)			
Piezo1 AC	—	Piezo1 AC	7.92
Piezo2 AC	9.06	Piezo2 AC	7.57
Piezo3 AC	6.97	Piezo3 AC	8.00
Bottom water AC	6.72	Bottom water AC	−1.15
Piezometer (DR)			
Piezo1a DR	—	Piezo1a DR	7.02
Piezo2a DR	—	Piezo2a DR	10.10
Piezo3a DR	12.87	Piezo3a DR	9.92
Bottom water DR	9.09	Bottom water DR	0.17

HCO_3 (Zhou et al., 2017). (Figure 8a,b) both indicate and confirm the isotope indicator suggestions that groundwater hydrochemistry was primarily influenced by both silicate weathering and carbonate dissolution (Gaillardet et al., 1999; Xiao et al., 2015; Zhu et al., 2011), which is reflected in the geological composition of the aquifers within the Lough Gur catchment comprising of volcanic and carbonate rocks (Ball, 2004).

The plot of (Ca^{2+} + Mg^{2+}) versus (HCO_3^- + SO_4^{2-}) (Figure 8c) illustrates that all groundwater samples fall below the 1:1 line over both hydroperiods, which further indicates that the dissolution of both carbonate and silicate are the main sources of Ca^{2+} and Mg^{2+} in catchment groundwater (Lakshmanan et al., 2003; Zhang et al., 2020).

The plot of (Cl^- + SO_4^{2-}) versus HCO_3^- (Figure 8d) shows that groundwater samples under low flow conditions mainly plot above the 1:1 line, indicating that carbonate dissolution may be the

dominant material source of the chemical composition of this groundwater. In contrast, groundwater samples under high flow conditions plot on both sides of the 1:1 line, indicating both carbonate dissolution and silicate weathering are the main material sources of the hydro-chemical composition of groundwater (Zhou et al., 2017).

Once the geological composition of a catchment contains Mg-bearing minerals such as dolomite, Mg^{2+} concentrations may perform as a reliable groundwater residence time indicator (Appelo & Postma, 2005; Morse & Mackenzie, 1990). Overall Mg/Ca ratios in surface and groundwaters are higher for low flow periods than high flow periods (Figure S2) as there is more time for water rock interaction, mineral dissolution and accumulation of infiltrating solutes (Luo et al., 2016).

An indicator of cation sources associated with silicate weathering is the milligram equivalent ratio of [(Na^+ + K^+)/Cl^-], where a ratio
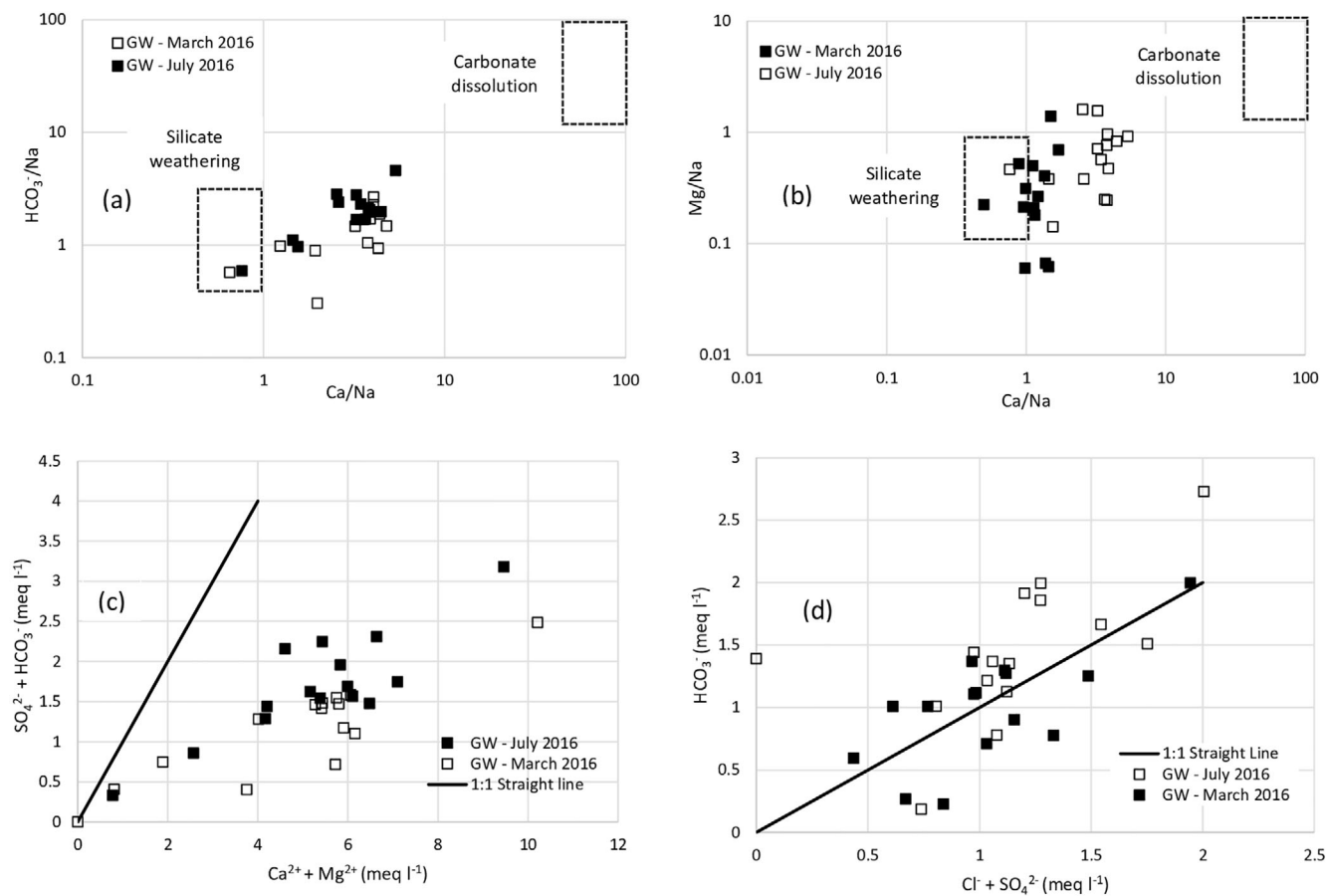
FIGURE 8 Bivariate plots of molar ratio (mmol L^{-1}] (a) Na-normalized Ca versus Na-normalized HCO_3^-, (b) Na-normalized Mg, and bivariate plots of ionic relations (meq l^{-1}) (c) $Ca^{2+} + Mg^{2+}$ versus $HCO_3^- + SO_4^{2-}$ and (d) $Cl^- + SO_4^{2-}$ versus HCO_3^-.

greater than 1 indicates release of cations from silicate weathering and a ratio of 1 or less suggests dissolution from other geological materials (Mukherjee & Fryar, 2008; Zhou et al., 2017) (Figure S3).

3.7 | Carbonate weathering processes and dissolved inorganic carbon

The biogeochemical processes responsible for the sources of DIC from geological materials have characteristic carbon isotope signatures and molar geochemical ratios which in karst aquifers may be particularly useful as a tracer for DIC and associated groundwater evolution (Cane & Clark, 1999; Clark & Fritz, 1997; Zhao et al., 2015). Sources of DIC in surface and groundwaters generally have three primary sources, atmospheric CO_2, CO_2 from organic matter mineralization and carbonate dissolution (Han et al., 2010). The mechanisms involved in DIC production are outlined by the equations in Equations S1–S4.

In this study the values for $\delta^{13}C_{DIC}$ in groundwater samples are seasonally dynamic being −16.9‰ under high flow periods and −15‰ under low flow periods (Figure 9c). This variation may be

due to isotopic fractionation induced by high respiration rates and molecular diffusion of CO_2 through soil pores during the summer months (Amiotte-Suchet et al., 1999; Cane & Clark, 1999). Seasonal variation is significant ($p < 0.01$) which may suggest that the contribution processes of biogenic DIC are seasonally different. The two primary processes in this study likely to be causing such seasonal variation in karst groundwater $\delta^{13}C_{DIC}$ signatures are: (1) soil CO_2 generated by plant respiration and microbial activities at higher temperatures during summer periods, and (2) faster soil CO_2 recharge to groundwater with more frequent rain events during high flow periods (Li et al., 2010a).

Correlations between $\delta^{13}C_{DIC}$ and DOC gives additional information on the source of DIC to surface and groundwaters (Figure 9). Positive correlation between $\delta^{13}C_{DIC}$ and DOC implies that oxidation of organic matter was a source of DIC while a negative correlation may suggest DIC is derived from dissolution of carbonate minerals by carbonic acids in the system (Li et al., 2010b). The $\delta^{13}C_{DIC}$ signatures from the in-lake piezometers (Figure 9a,b) at Lough Gur under high and low flow conditions suggest oxidation of organic matter is the likely source of DIC (Han et al., 2010). For groundwater samples (Figure 9c) there is a slight positive

FIGURE 9 Variation of $\delta^{13}C_{DIC}$ (‰) with DOC for (a) lake-bed piezometer and bottom waters, (b) surface water and (c) groundwater samples collected from the lough Gur catchment during high flow (March 2016) and low flow (July 2016) periods.
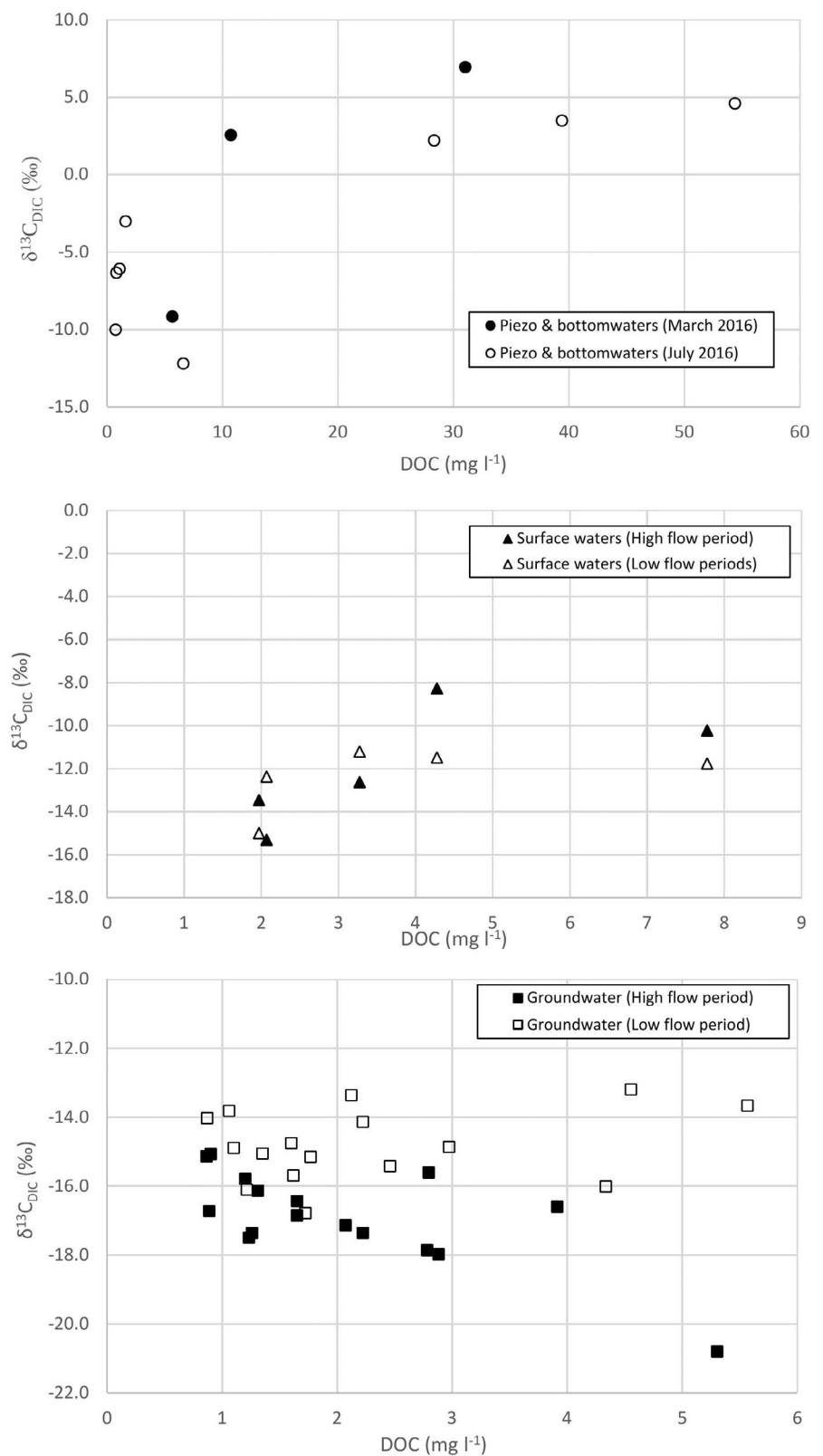
correlation under low flow conditions while under high flow conditions there is a negative correlation which would suggest a seasonal switch in the source of DIC from oxidation of organic matter (from surface recharge) towards dissolution of carbonate in the aquifer under longer residence times.

3.8 | Groundwater and surface-water CO$_2$ evasion to the atmosphere

The loss of DIC from surface and groundwaters in karstic environments is mainly caused by uptake by aquatic plants, calcite or
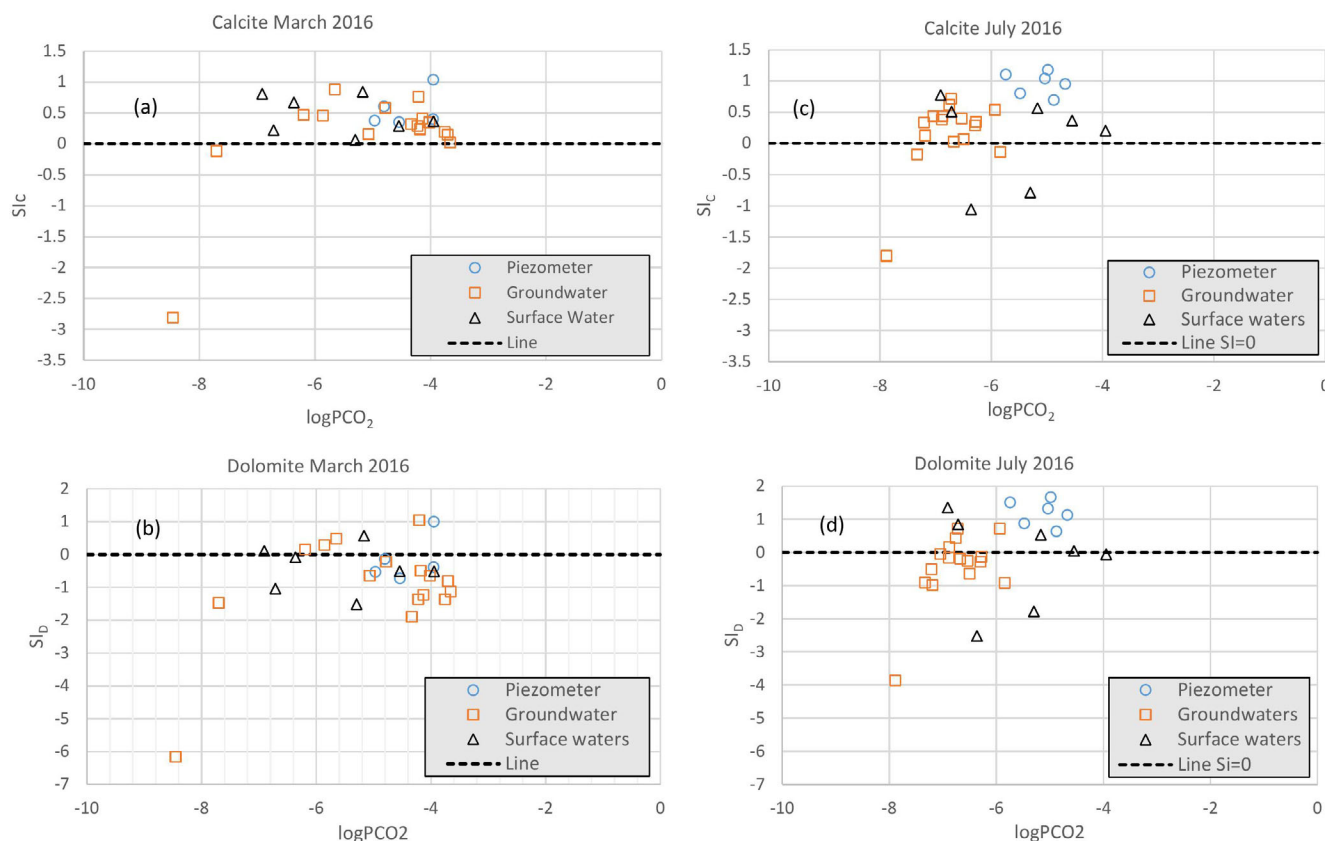
FIGURE 10 Calcite (SIC) and dolomite (SID) saturation index for water collected from piezometers and bottom waters, groundwater and surface waters from the lough Gur catchment under high flow (a, b) and low flow (c, d) conditions. The dashed line represents SI = 0.

dolomite precipitation and potentially CO_2 evasion to the atmosphere (Sironić et al., 2017; Zhao et al., 2015). The partial pressure of carbon dioxide (pCO_2) in groundwaters is a function of soil respiration, which increases pCO_2 and dissolution of carbonate minerals. pCO_2, calcite (SI_C) and dolomite (SI_D) saturation ratio are calculated according to chemical equilibrium equations (Clark & Fritz, 1997). The SI saturation for calcite (SI_C) is above 0 and seasonally consistent for the majority of water compartments for both hydroperiods in the Lough Gur catchment which means it is supersaturated Figure 10. This indicates that calcium carbonate precipitation occurs which results in CO_2 evasion for most water samples as the pCO_2 is higher than atmospheric (Martinsen et al., 2020; Shin et al., 2011). Furthermore, during high flow periods many water compartments are super-saturated for calcite and under-saturated for dolomite which suggests dolomite dissolution to be a source of Ca^{2+}, Mg^{2+} and HCO_3^- particularly during periods of recharge (Han et al., 2010; Szramek et al., 2007; Yu et al., 2021). Under low flow conditions the elevated source of Mg^{2+} (Figure 10) may be due to the partial dissolution of dolomite and accumulation of Mg^{2+} due to incongruent weathering (Edmunds & Shand, 2009).

The $\delta^{13}C_{DIC}$ (‰) and pCO_2 signatures (Figure S4) for the lakebed piezometer PZ-1 indicates the perennial source of DIC to be carbonate weathering by acids other than carbonic acid or soil CO_2 which may be due to the influence from the nearby volcanic tuft layer covering the Waulsortian and Lough Gur limestone layers. In contrast, DIC sources at the PZ-2 piezometer location indicate carbonate weathering is perennially dominated by soil CO_2 (Li et al., 2010a). Surface water $\delta^{13}C_{DIC}$ (‰) and pCO_2 signatures indicate carbonate weathering by carbonic acid from soil CO_2 is the dominant carbon mobilization process during low flow periods. Concurrently, the lower DIC concentrations in surface waters during low flow indicates CO_2 efflux and consumption fuelling biogeochemical reactions and function (i.e., algal productivity) (Martinsen et al., 2020). In contrast, the higher DIC concentrations in groundwaters and piezometers which are perennially in equilibrium with soil CO_2 may be as a result of increased contact time and microbial activity, in addition to higher soil CO_2 concentrations (Han et al., 2010; Li et al., 2010b).

3.9 | Relationship between carbonate chemistry with soil nitrate

Following application of N containing fertilizer and manure, ammonium (NH_4^+) in the form of NH_4NO_3, $(NH_4)_2SO_4$, $(CO[NH_2]_2)$, NH_3 and $([NH_4]_2PO_4)$ undergoes in-soil nitrification in a two step oxidation process by autotrophic bacteria involving *Nitrosomonas*, *Nitrobacter* and *Nitropsira* sp. to generate bioavailable nitrate (NO_3^-) (Berthelin et al., 1985).

N-fertilizer and manure applications in agricultural catchments increase nitrogen sources in soils which (Equations S5 and S6), when nitrified produce hydrogen ions (H^+) which contribute to carbonate dissolution (Equations S1–S4). Once protons from this nitrification process are added to the system, there is an increase in the Ca^{2+} and Mg^{2+} concentration which will equilibrate with nitrate anions. Consequently, HCO_3^- will decrease due to transformation to CO_2 gas phase and is released into the soil/atmosphere (Perrin et al., 2008a). The overall dissolution of carbonate rocks by nitric acid produced by nitrification processes may be described by Equation (1):

$$(Ca_{1-x}Mg_x)CO_3 + NH_4NO_3 + 2O_2 \\ \rightarrow (1-x)Ca^{2+} + xMg^{2+} + 2NO_3^- + 2H_2O + CO_2 \qquad (2)$$
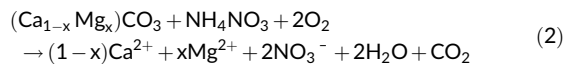
The source of acidity leading to the weathering processes is related to the molar ratio $(Ca^{2+} + Mg^{2+})/HCO_3^-$ (Figure 11a). In groundwater wells and boreholes, the molar ratio between $(Ca^{2+} + Mg^{2+})$ and HCO_3^- ions released into groundwater decreases slightly from 2.8 to 1.9 between the high flow to low flow period. Both ratios are above 0.5 which has been used to represent a system which is disturbed by proton inputs from nitrification of N-fertilizers and manures (Perrin et al., 2008a). The lower ratio indicates carbonic acid carbonate dissolution natural weathering, while the increased ratio up to 2.8 during the higher flow period indicates that carbonic acid is not the only weathering chemical present.

Figure 11b shows the relationship between $\delta^{13}C_{DIC}$ and $[NO_3^-]/[HCO_3^-]$ molar ratios for water collected from groundwater, surface water and piezometer nests in the Lough Gur catchment under high and low flow conditions. Piezometer $\delta^{13}C_{DIC}$ signatures over both hydroperiods are between −8 and +6 suggesting carbonate weathering by another route other than carbonic acid. Organic matter degradation produces organic acids which can accelerate carbonate weathering (Li et al., 2010a)., however at some piezometers in the lake bed sediments (PZ-1) organic acid production may not be sufficient enough to activate effective carbonate weathering. Notably, the low $[NO_3^-]/[HCO_3^-]$ molar ratios in PZ-1 and PZ-2 suggest carbonate mineral dissolution is not associated with nitric acid but more related with carbonic acid.

The data distribution in Figure 11b suggests three component mixing with some overlaps for various aquatic compartments. The surface and groundwater locations with high $[NO_3^-]/[HCO_3^-]$ molar ratios and $\delta^{13}C_{DIC}$ between −13.0 and −18.0‰ indicate its carbonate chemistry is impacted by nitrate applications (Liu et al., 2006). Previous studies have illustrated that stable isotopes ($\delta^{15}N_{NO3-}$ and $\delta^{18}O_{NO3-}$) of nitrate may be successfully used to elucidate the sources and transformations of NO_3 in water samples based on distinctive source isotopic signatures (Panno et al., 2006) Figure 11c shows the relationship between $\delta^{18}O_{NO3-}$ and $\delta^{15}N_{NO3-}$ for groundwater samples in the Lough Gur catchment. The origin of nitrate to groundwater in the catchment from these isotopic signatures suggest manure and/or domestic effluent being the primary source (Yue et al., 2015a).

3.10 | Conceptual hydrogeological and (bio)geochemical processes model

A hydrogeological conceptual model of the Lough Gur catchment was developed which enables an accurate visualization of the prevailing groundwater flow direction, in-lake groundwater discharge locations as well as the seasonally dynamic hydrological processes discussed in previous sections which influence the hydrological and biogeochemical function of the lake (Figure 12a).

Geophysical surveys, dye tracing experiments and water isotopic signatures confirmed the perennially active conduit flow path from the lake swallow hole "Pollavadra" to the discharge springs (SW-2 and SW-3) which follows the bedding plane between the Waulsortian limestone and the Lough Gur formation. Water infiltrates the Knockroe volcanic formations overlying the Lough Gur and Waulsortian limestone formations which flows towards the lake. Variations in the seasonal connectivity between surface water and surrounding catchment groundwaters were highlighted by the branching out of the local evaporation line (LEL) under high flow conditions suggesting a tighter coupling between groundwater and surface-water when water is abundant (Stroj et al., 2020). Elevated groundwater levels activate upper karst conduits in the original unsaturated zone which results in complex flowpaths and increased water source connectivity. Under low flow this intersection occurs some distance down the water flow path indicating it takes more time to see groundwater at the surface during these periods (Rusjan et al., 2019). Additionally, water isotope signatures indicate there is a disconnection between upper and low karst conduits resulting in less groundwater surface-water interaction.

From the conceptual model, in-lake spring discharge locations are highlighted along with the low permeability lake-bed sediments (Figure 12a). The upper Lough Gur and Waulsortian limestone formations have well developed vertical and horizontal fissures with the general direction related to the prevailing groundwater flow. Generally, despite the overlying Knockroe formations, fast flow is evident to the lake under high flow conditions resulting from rapid infiltration and recharge through karst conduits from the rapid response of groundwater levels at the elevated eastern side of the lake. In particular, rainfall infiltration and recharge through the Knockroe volcanic and limestone conduits to the east of the lake may result in dolomite under-saturation, which suggests this to be an important mineralization process and source of Mg^{2+} to associated water compartments (Figure 12a).

Stable isotopes of water and d-excess values particularly illustrate seasonal and spatial dynamics in groundwater evolution, recharge processes and flow pathways to and from the lake between water compartments. Significantly, $\delta^{18}O$ and δ^2H signatures for groundwaters plot above the GMWL and LMWL lines indicating (de)hydration of silicate minerals and direct isotope exchange of $\delta^{18}O$ between water and rock minerals (Allegre, 2008; Brkić et al., 2016). This highlights the potential importance of such geochemical processes for groundwater hydro-chemical composition in karst/volcanic aquifer systems (Figure 12b).
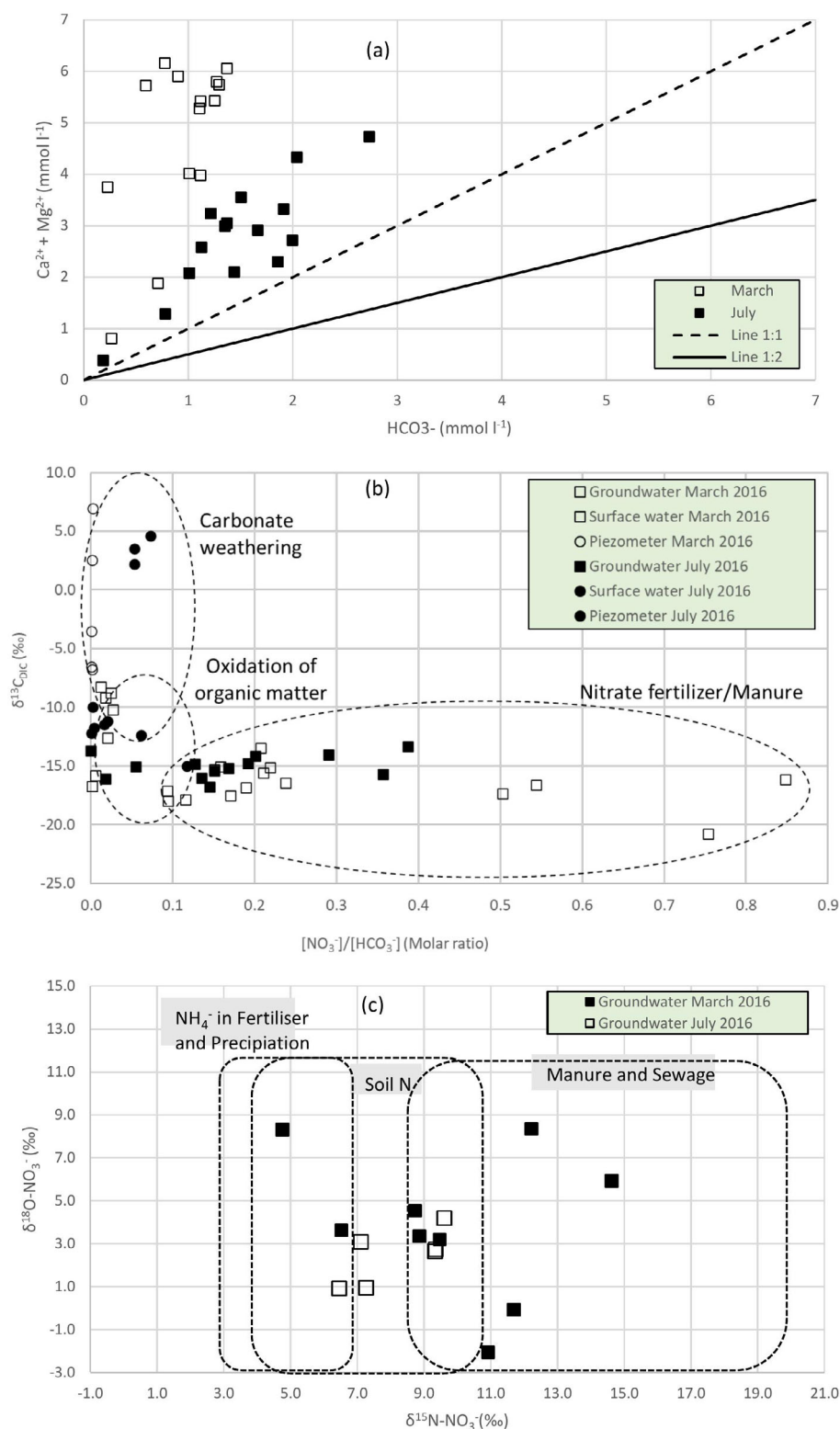
FIGURE 11 (a) Relationship between $(Ca^{2+}+Mg^{2+})$ and HCO_3^- concentrations in groundwater samples from the Lough Gur catchment; and (b) Plot showing relationship between $\delta^{13}C_{DIC}$ and $(NO_3^-)/(HCO_3^-)$ molar ratios for water collected from groundwater, surface water and piezometer nests in the Lough Gur catchment under high (March 2016) and low flow (July 2016) conditions; and (c) Relationship between $\delta^{18}O-NO_3^-$ and $\delta^{15}N-NO_3^-$ in groundwater samples from the Lough Gur catchment.

The primary biogeochemical and geochemical processes associated with carbon and nitrogen cycling within this geologically heterogeneous groundwater-fed lake catchment are illustrated in Figure 13. Spatial variation for nitrate isotopic signatures (e.g., $\delta^{18}O_{NO3-}$ and $\delta^{15}N_{NO3-}$) suggest a number of potential nitrate sources to groundwaters including soil organic nitrogen, manure and/or domestic effluent with indications of denitrification processes under low flow conditions. The primary nitrification processes include nitrate liberation from ammonium and ammonium nitrate while denitrification processes involve degradation of organic matter under more anoxic conditions as outlined in Figure 13.
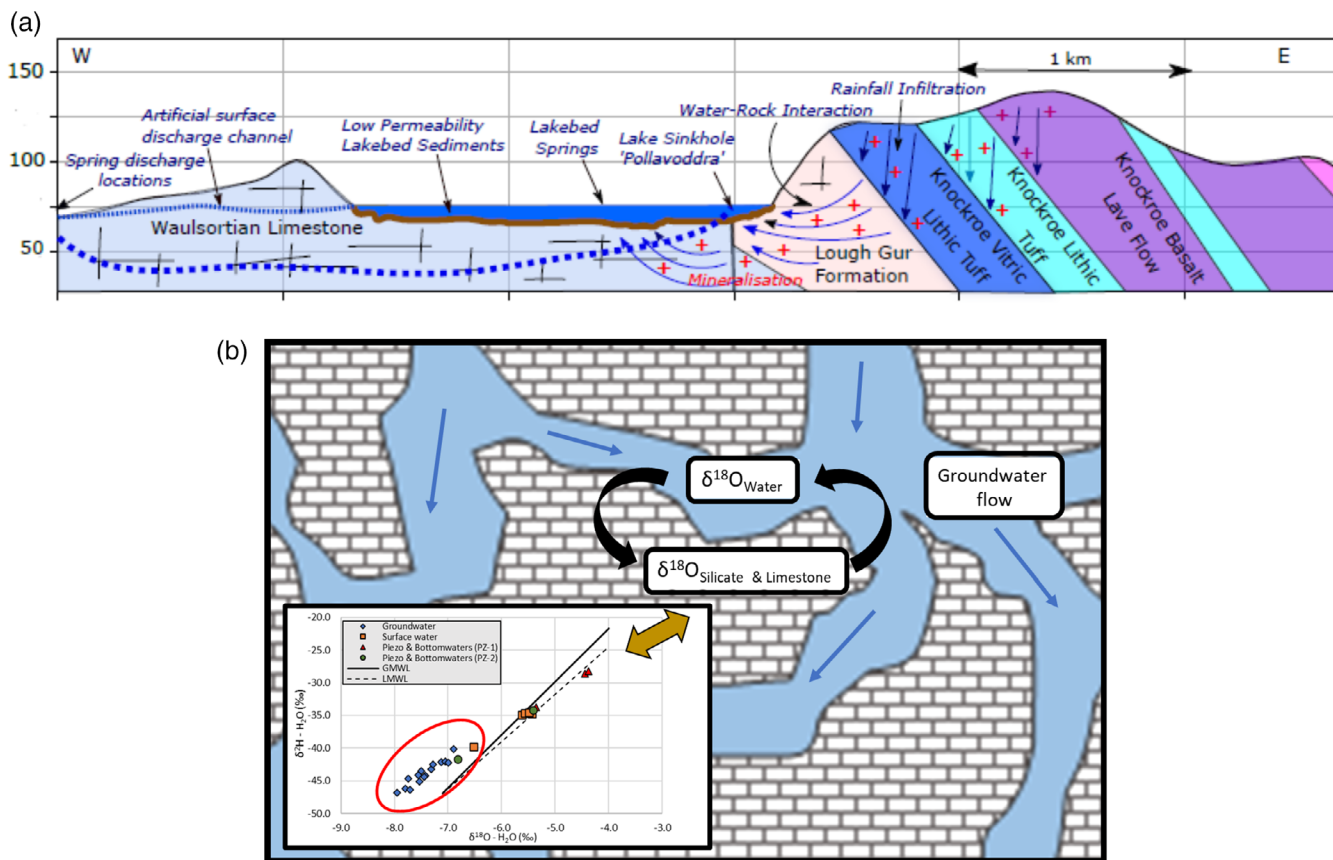
FIGURE 12 (a) Schematic conceptual hydrogeological cross-section of the Lough Gur multi-layer aquifer system showing the prevailing groundwater flow direction from E to W with elevations in meters over datum (mOD); (b) Isotope exchange of $\delta^{18}O$ between water and the mineral crystal lattice during contact with flowing groundwater in fractures and faults characterized by signatures above the GMWL.
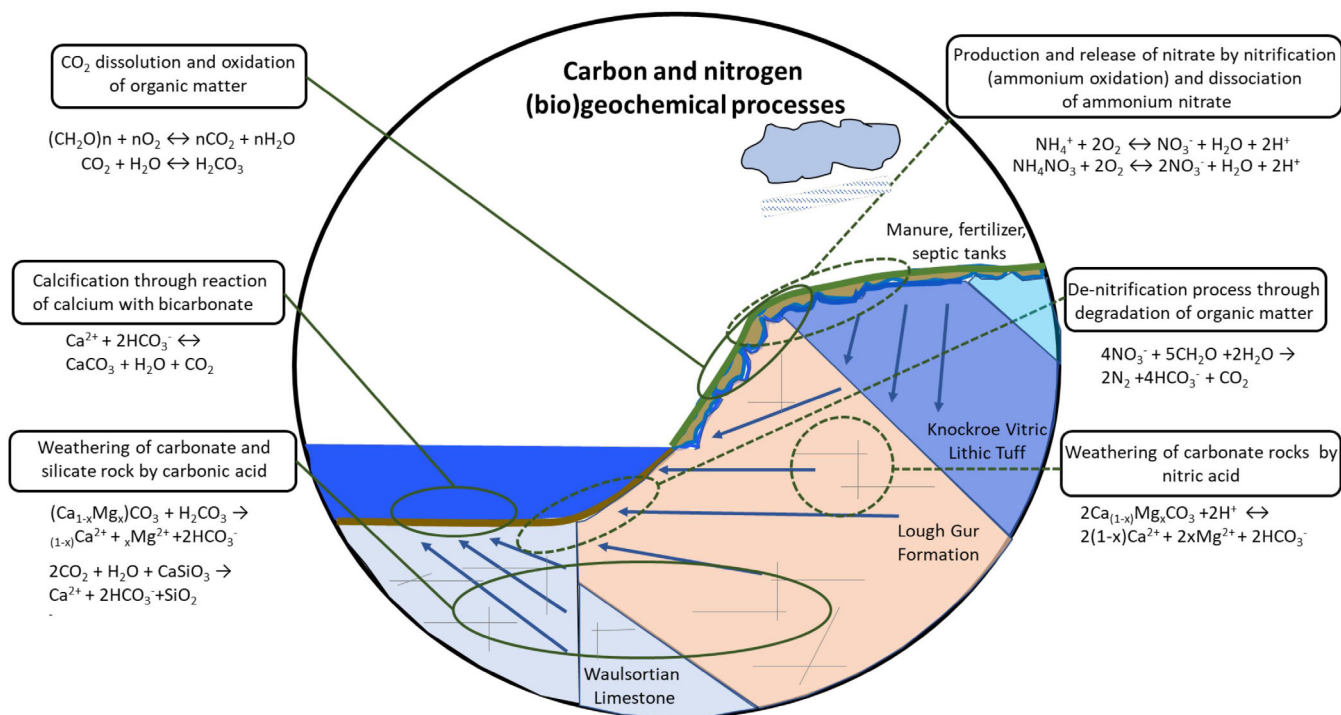

FIGURE 13 Summary of the major carbonate and nitrogen (bio)geochemical processes within the Lough Gur multi-layer aquifer system.

Geochemical indicators suggest carbonate weathering processes through the reaction of dilute nitric acid and carbonate rocks. Such chemical weathering of carbonate rocks through nitrification and denitrification processes has been observed as an important (bio)geochemical process in similar small carbonate containing agricultural catchments (Perrin et al., 2008b; Yue et al., 2015b). Dissolution of CO_2 and oxidation of organic matter resulting in generation of dilute carbonic acid plays a pivotal role in carbonate weathering (Li et al., 2010b). Hydrochemistry and carbon isotopic compositions of dissolved inorganic carbon show groundwater carbon geochemistry is governed by a seasonal switch between carbonate weathering and oxidation of organic matter. Correlations between carbonate weathering parameters and pCO_2 indicate for the majority of water compartments, the partial pressure of soil CO_2 recharge is an important influencing recharge process Figure S5.

Overall, this study illustrates how the findings of complementary investigative methods can contribute detailed insights towards the development of conceptual hydrogeological and (bio)geochemical models for geologically heterogeneous aquifer systems.

DATA AVAILABILITY STATEMENT

The data that support the findings of this study are available on request from the corresponding author. The data are not publicly available due to privacy or ethical restrictions.

ORCID

David W. O'Connell https://orcid.org/0000-0002-1974-8145

REFERENCES

Ala-aho, P., Soulsby, C., Pokrovsky, O. S., Kirpotin, S. N., Karlsson, J., Serikova, S., Vorobyev, S. N., Manasypov, R. M., Loiko, S., & Tetzlaff, D. (2018). Using stable isotopes to assess surface water source dynamics and hydrological connectivity in a high-latitude wetland and permafrost influenced landscape. *Journal of Hydrology*, *556*, 279–293. https://doi.org/10.1016/j.jhydrol.2017.11.024

Allegre, C. J. (2008). *Isotope geology*. Cambridge University Press.

Amiotte-Suchet, P., Aubert, D., Probst, J. L., Gauthier-Lafaye, F., Probst, A., Andreux, F., & Viville, D. (1999). δ13C pattern of dissolved inorganic carbon in a small granitic catchment: The Strengbach case study (Vosges mountains, France). *Chemical Geology*, *159*(1–4), 129–145. https://doi.org/10.1016/S0009-2541(99)00037-6

Appelo, C., & Postma, D. (2005). *Geochemistry, groundwater and pollution*. CRC.

Ball, D. (2004). *Lough Gur – Hydrological assessment draft report*. Limerick County Council.

Berthelin, J., Bonne, M., Belgy, G., & Wedraogo, F. X. (1985). A major role for nitrification in the weathering of minerals of brown acid forest soils. *Geomicrobiology Journal*, *4*(2), 175–190. https://doi.org/10.1080/01490458509385930

Bowen, G. J., Putman, A., Brooks, J. R., Bowling, D. R., Oerter, E. J., & Good, S. P. (2018). Inferring the source of evaporated waters using stable H and O isotopes. *Oecologia*, *187*(4), 1025–1039. https://doi.org/10.1007/s00442-018-4192-5

Brkić, Ž., Briški, M., & Marković, T. (2016). Use of hydrochemistry and isotopes for improving the knowledge of groundwater flow in a semiconfined aquifer system of the eastern Slavonia (Croatia). *Catena*, *142*, 153–165. https://doi.org/10.1016/j.catena.2016.03.010

Burnett, W. C., Peterson, R., Moore, W. S., & de Oliveira, J. (2008). Radon and radium isotopes as tracers of submarine groundwater discharge - results from the Ubatuba, Brazil SGD assessment intercomparison. *Estuarine, Coastal and Shelf Science*, *76*(3), 501–511. https://doi.org/10.1016/j.ecss.2007.07.027

Cane, G., & Clark, I. D. (1999). Tracing ground water recharge in an agricultural watershed with isotopes. *Ground Water*, *37*(1), 133–139. https://doi.org/10.1111/j.1745-6584.1999.tb00966.x

Chen, X., Zhang, Z., Soulsby, C., Cheng, Q., Binley, A., Jiang, R., & Tao, M. (2018). Characterizing the heterogeneity of karst critical zone and its hydrological function: An integrated approach. *Hydrological Processes*, *32*(19), 2932–2946. https://doi.org/10.1002/hyp.13232

Cherkauer, D. S., & Nader, D. C. (1989). Distribution of groundwater seepage to large surface-water bodies: The effect of hydraulic heterogeneities. *Journal of Hydrology*, *109*(1–2), 151–165. https://doi.org/10.1016/0022-1694(89)90012-7

Claerbout, J. F., & Muir, F. (1973). Robust modeling with erratic data. *Geophysics*, *38*(5), 826–844.

Clark, I. D., & Fritz, P. (1997). Environmental isotopes in hydrogeology. *Environmental Isotopes in Hydrogeology*.

Coggon, J. H. (1971). Electromagnetic and electrical modeling by the finite element method. *Geophysics*, *36*(1), 132–155.

Comte, J.-C., Cassidy, R., Nitsche, J., Ofterdinger, U., Pilatova, K., & Flynn, R. (2012). The typology of Irish hard-rock aquifers based on an integrated hydrogeological and geophysical approach. *Hydrogeology Journal*, *20*(8), 1569–1588. https://doi.org/10.1007/s10040-012-0884-9

Coplen, T. B. (2011). Idelines and recommended terms for expression of stable-isotope-ratio and gas- ratio measurement results. *Rapid Communications in Mass Spectroscopy*, *25*, 2538–2560.

Cui, B.-L., & Li, X.-Y. (2015). Runoff processes in the Qinghai Lake Basin, Northeast Qinghai-Tibet plateau, China: Insights from stable isotope and hydrochemistry. *Quaternary International*, *380–381*, 123–132. https://doi.org/10.1016/j.quaint.2015.02.030

Dahlin, T., & Zhou, B. (2004). A numerical comparison of 2D resistivity imaging with 10 electrode arrays. *Geophysical Prospecting*, *52*(5), 379–398. https://doi.org/10.1111/j.1365-2478.2004.00423.x

Dar, F. A., Jeelani, G., Perrin, J., & Ahmed, S. (2021). Groundwater recharge in semi-arid karst context using chloride and stable water isotopes. *Groundwater for Sustainable Development*, *14*, 100634. https://doi.org/10.1016/j.gsd.2021.100634

Deakin J, Daly D, Coxon C. 1998. County Limerick groundwater protection scheme. Main report.

Diefendorf, A. F., & Patterson, W. P. (2005). Survey of stable isotope values in Irish surface waters. *Journal of Paleolimnology*, *34*(2), 257–269. https://doi.org/10.1007/s10933-005-3571-1

Doctor, D. H., Jr., Alexander, E. C., Jr., Petrič, M., Kogovšek, J., Urbanc, J., Lojen, S., & Stichler, W. (2006). Quantification of karst aquifer discharge components during storm events through end-member mixing analysis using natural chemistry and stable isotopes as tracers. *Hydrogeology Journal*, *14*(7), 1171–1191. https://doi.org/10.1007/s10040-006-0031-6

Edmunds, W. M., & Shand, P. (2009). *Natural groundwater quality*. John Wiley & Sons.

Fellows, C. R., & Brezonik, P. L. (1980). Seepage flow into Florida lakes. *Journal of the American Water Resources Association*, 16(4), 635–641. https://doi.org/10.1111/j.1752-1688.1980.tb02442.x

Gaillardet, J., Dupré, B., Louvat, P., & Allègre, C. J. (1999). Global silicate weathering and CO2 consumption rates deduced from the chemistry of large rivers. *Chemical Geology*, 159(1–4), 3–30. https://doi.org/10.1016/S0009-2541(99)00031-5

Gat, J. R., & Matsui, E. (1991). Atmospheric water balance in the Amazon Basin: An isotopic evapotranspiration model. *Journal of Geophysical Research*, 96(D7), 13179–13188. https://doi.org/10.1029/91jd00054

Gautam, M. K., Lee, K.-S., & Song, B.-Y. (2018). Characterizing groundwater recharge using oxygen and hydrogen isotopes: A case study in a temperate forested region, South Korea. *Environmental Earth Sciences*, 77(3), 110. https://doi.org/10.1007/s12665-018-7279-8

Geotomo Software. (2010). Instruction manual for Res3DInv x64, version 3.01: Rapid 3D resistivity and IP inversion using the least-squares method. http://www.geoelectrical.com/downloads.php. Accessed 25 May 2022.

Gibson, J. J., Birks, S. J., Jeffries, D., & Yi, Y. (2017). Regional trends in evaporation loss and water yield based on stable isotope mass balance of lakes: The Ontario Precambrian shield surveys. *Journal of Hydrology*, 544, 500–510. https://doi.org/10.1016/j.jhydrol.2016.11.016

Gibson, J. J., Birks, S. J., Yi, Y., Moncur, M. C., & McEachern, P. M. (2016). Stable isotope mass balance of fifty lakes in Central Alberta: Assessing the role of water balance parameters in determining trophic status and lake level. *Journal of Hydrology: Regional Studies*, 6, 13–25. https://doi.org/10.1016/j.ejrh.2016.01.034

Gibson, J. J., Prepas, E. E., & McEachern, P. (2002). Quantitative comparison of lake throughflow, residency, and catchment runoff using stable isotopes: Modelling and results from a regional survey of boreal lakes. *Journal of Hydrology*, 262(1–4), 128–144. https://doi.org/10.1016/S0022-1694(02)00022-7

Gil-Márquez, J. M., Andreo, B., & Mudarra, M. (2019). Combining hydrodynamics, hydrochemistry, and environmental isotopes to understand the hydrogeological functioning of evaporite-karst springs. An example from southern Spain. *Journal of Hydrology*, 576, 299–314. https://doi.org/10.1016/j.jhydrol.2019.06.055

Guo, Y., Qin, D., Li, L., Sun, J., Li, F., & Huang, J. (2019). A complicated karst spring system: Identified by karst springs using water level, hydrogeochemical, and isotopic data in Jinan, China. *Water (Switzerland)*, 11(5), 947. https://doi.org/10.3390/w11050947

Halder, J., Decrouy, L., & Vennemann, T. W. (2013). Mixing of Rhône River water in Lake Geneva (Switzerland-France) inferred from stable hydrogen and oxygen isotope profiles. *Journal of Hydrology*, 477, 152–164. https://doi.org/10.1016/j.jhydrol.2012.11.026

Hampton, T. B., Zarnetske, J. P., Briggs, M. A., Singha, K., Harvey, J. W., Day-Lewis, F. D., MahmoodPoor Dehkordy, F., & Lane, J. W. (2019). Residence time controls on the fate of nitrogen in flow-through lakebed sediments. *Journal of Geophysical Research – Biogeosciences*, 124(3), 689–707. https://doi.org/10.1029/2018JG004741

Han, G., Tang, Y., & Wu, Q. (2010). Hydrogeochemistry and dissolved inorganic carbon isotopic composition on karst groundwater in Maolan, Southwest China. *Environmental Earth Sciences*, 60(4), 893–899. https://doi.org/10.1007/s12665-009-0226-y

Hickey, C. (2010). The use of multiple techniques for conceptualisation of lowland karst, a case study from county Roscommon, Ireland. *Acta Carsologica*, 39(2), 331–346. https://doi.org/10.3986/ac.v39i2.103

Hitzman, M. W., Redmond, P. B., & Beaty, D. W. (2002). The carbonate-hosted Lisheen Zn-Pb-ag deposit, county Tipperary, Ireland. *Economic Geology*, 97(8), 1627–1655. https://doi.org/10.2113/gsecongeo.97.8.1627

Huang, P., & Wang, X. (2018). Groundwater-mixing mechanism in a multi-aquifer system based on isotopic tracing theory: A case study in a coal Mine District, China. *Geofluids*, 2018, 1–10. https://doi.org/10.1155/2018/9549141

Jasechko, S., Birks, S. J., Gleeson, T., Wada, Y., Fawcett, P. J., Sharp, Z. D., McDonnell, J. J., & Welker, J. M. (2014). The pronounced seasonality of global groundwater recharge. *Water Resources Research*, 50(11), 8845–8867. https://doi.org/10.1002/2014WR015809

Jiang, R., Bao, Y., Shui, Y., Wang, Y., Hu, M., Cheng, Y., Cai, A., Du, P., & Ye, Z. (2018). Spatio-temporal variations of the stable H-O isotopes and characterization of mixing processes between the mainstream and tributary of the three gorges reservoir. *Water (Switzerland)*, 10(5), 563. https://doi.org/10.3390/w10050563

Johnsen, S. J., Dansgaard, W., & White, J. W. C. (1989). The origin of Arctic precipitation under present and glacial conditions. *Tellus Series B*, 41B(4), 452–468. https://doi.org/10.3402/tellusb.v41i4.15100

Kamtchueng, B. T., Fantong, W. Y., Wirmvem, M. J., Tiodjio, R. E., Fouépé Takounjou, A., Asai, K., Bopda Djomou, S. L., Kusakabe, M., Ohba, T., Tanyileke, G., Hell, J. V., & Ueda, A. (2015). A multi-tracer approach for assessing the origin, apparent age and recharge mechanism of shallow groundwater in the Lake Nyos catchment, northwest, Cameroon. *Journal of Hydrology*, 523, 790–803. https://doi.org/10.1016/j.jhydrol.2015.02.008

Käser, D. H., Binley, A., Heathwaite, A. L., & Krause, S. (2009). Spatio-temporal variations of hyporheic flow in a riffle-step-pool sequence. *Hydrological Processes*, 23(15), 2138–2149. https://doi.org/10.1002/hyp.7317

Katz, B. G., & Bullen, T. D. (1996). The combined use of 87Sr/86Sr and carbon and water isotopes to study the hydrochemical interaction between groundwater and lakewater in mantled karst. *Geochimica et Cosmochimica Acta*, 60(24), 5075–5087. https://doi.org/10.1016/S0016-7037(96)00296-7

Kazmierczak, J., Müller, S., Nilsson, B., Postma, D., Czekaj, J., Sebok, E., Jessen, S., Karan, S., Stenvig Jensen, C., Edelvang, K., & Engesgaard, P. (2016a). Groundwater flow and heterogeneous discharge into a seepage lake: Combined use of physical methods and hydrochemical tracers. *Water Resources Research*, 52(11), 9109–9130. https://doi.org/10.1002/2016WR019326

Kazmierczak, J., Müller, S., Nilsson, B., Postma, D., Czekaj, J., Sebok, E., Jessen, S., Karan, S., Stenvig Jensen, C., Edelvang, K., & Engesgaard, P. (2016b). Groundwater flow and heterogeneous discharge into a seepage lake: Combined use of physical methods and hydrochemical tracers. *Water Resources Research*, 52(11), 9109–9130. https://doi.org/10.1002/2016WR019326

Kidmose, J., Engesgaard, P., Nilsson, B., Laier, T., & Looms, M. C. (2011). Spatial distribution of seepage at a flow-through Lake: Lake Hampen, western Denmark. *Vadose Zone Journal*, 10(1), 110–124. https://doi.org/10.2136/vzj2010.0017

Kidmose, J., Engesgaard, P., Ommen, D. A. O., Nilsson, B., Flindt, M. R., & Andersen, F. O. (2015). The role of groundwater for Lake-water quality and quantification of N seepage. *Groundwater*, 53(5), 709–721. https://doi.org/10.1111/gwat.12281

Kidmose, J., Nilsson, B., Engesgaard, P., Frandsen, M., Karan, S., Landkildehus, F., Søndergaard, M., & Jeppesen, E. (2013). Focused groundwater discharge of phosphorus to a eutrophic seepage Lake (lake Væng, Denmark): Implications for lake ecological state and restoration. *Hydrogeology Journal*, 21(8), 1787–1802. https://doi.org/10.1007/s10040-013-1043-7

Kishel, H. F., & Gerla, P. J. (2002). Characteristics of preferential flow and groundwater discharge to Shingobee Lake, Minnesota, USA. *Hydrological Processes*, 16(10), 1921–1934. https://doi.org/10.1002/hyp.363

Kovačič, G., & Ravbar, N. (2010). Extreme hydrological events in karst areas of Slovenia, the case of the Unica River basin. *Geodinamica Acta*, 23(1–3), 89–100. https://doi.org/10.3166/ga.23.89-100

Krabbenhoft, D. P., Bowser, C. J., Anderson, M. P., & Valley, J. W. (1990). Estimating groundwater exchange with lakes: 1. The stable isotope

mass balance method. *Water Resources Research*, 26(10), 2445–2453. https://doi.org/10.1029/WR026i010p02445

Lakshmanan, E., Kannan, R., & Kumar, M. S. (2003). Major ion chemistry and identification of hydrogeochemical processes of ground water in a part of Kancheepuram district, Tamil Nadu, India. *Environmental Geosciences*, 10(4), 157–166. https://doi.org/10.1306/eg.0820303011

Langford, R., & Gill, M. (2016). *Lough Gur catchment study report*. Parkmore Environmental Services.

Layden NM (1993). A limnological study of Lough Gur, County Limerick. Trinity College Dublin.

Li, S.-L., Liu, C.-Q., Li, J., Lang, Y.-C., Ding, H., & Li, L. (2010a). Geochemistry of dissolved inorganic carbon and carbonate weathering in a small typical karstic catchment of Southwest China: Isotopic and chemical constraints. *Chemical Geology*, 277(3–4), 301–309. https://doi.org/10.1016/j.chemgeo.2010.08.013

Li, S.-L., Liu, C.-Q., Li, J., Lang, Y.-C., Ding, H., & Li, L. (2010b). Geochemistry of dissolved inorganic carbon and carbonate weathering in a small typical karstic catchment of Southwest China: Isotopic and chemical constraints. *Chemical Geology*, 277(3–4), 301–309. https://doi.org/10.1016/j.chemgeo.2010.08.013

Lin, Z. (2011). Estimating water budgets and vertical leakages for Karst Lakes in North-Central Florida (United States) via hydrological modeling. *Journal of the American Water Resources Association*, 47(2), 287–302. https://doi.org/10.1111/j.1752-1688.2010.00513.x

Liu, C.-Q., Li, S.-A., Lang, Y.-C., & Xiao, H.-Y. (2006). Using $\delta^{15}N$- and $\delta^{18}O$-values to identify nitrate sources in karst ground water, Guiyang, Southwest China. *Environmental Science and Technology*, 40(22), 6928–6933. https://doi.org/10.1021/es0610129

Luo, M., Chen, Z., Criss, R. E., Zhou, H., Huang, H., Han, Z., & Shi, T. (2016). Dynamics and anthropogenic impacts of multiple karst flow systems in a mountainous area of South China. *Hydrogeology Journal*, 24(8), 1993–2002. https://doi.org/10.1007/s10040-016-1462-3

Luttenegger AL, DeGroot DJ. 1992. Measurement of hydraulic conductivity in clay using push in piezometers. Current practices in groundwater and vadose zone investigations. In ASTM 1118 Philadelphia.

Marfia, A. M., Krishnamurthy, R. V., Atekwana, E. A., & Panton, W. F. (2004). Isotopic and geochemical evolution of ground and surface waters in a karst dominated geological setting: A case study from Belize, Central America. *Applied Geochemistry*, 19(6), 937–946. https://doi.org/10.1016/j.apgeochem.2003.10.013

Martinsen, K. T., Kragh, T., & Sand-Jensen, K. (2020). Carbon dioxide efflux and ecosystem metabolism of small forest lakes. *Aquatic Sciences*, 82(1), 9. https://doi.org/10.1007/s00027-019-0682-8

McCormack, T., O'Connell, Y., Daly, E., Gill, L. W., Henry, T., & Perriquet, M. (2017). Characterisation of karst hydrogeology in Western Ireland using geophysical and hydraulic modelling techniques. *Journal of Hydrology: Regional Studies*, 10, 1–17. https://doi.org/10.1016/j.ejrh.2016.12.083

McCusker, J., & Reed, C. (2013). The role of intrusions in the formation of Irish-type mineralisation. *Mineralium Deposita*, 48(6), 687–695. https://doi.org/10.1007/s00126-013-0474-3

McIlvin, M. R., & Altabet, M. A. (2005). Chemical conversion of nitrate and nitrite to nitrous oxide for nitrogen and oxygen isotopic analysis in freshwater and seawater. *Analytical Chemistry*, 77(17), 5589–5595. https://doi.org/10.1021/ac050528s

Meinikmann, K., Lewandowski, J., & Hupfer, M. (2015). Phosphorus in groundwater discharge - a potential source for lake eutrophication. *Journal of Hydrology*, 524, 214–226. https://doi.org/10.1016/j.jhydrol.2015.02.031

Merlivat, L., & Jouzel, J. (1979). Global climatic interpretation of the deuterium-oxygen 16 relationship for precipitation. *Journal of Geophysical Research*, 84(C8), 5029–5033. https://doi.org/10.1029/JC084iC08p05029

Mitchell KL. 2014. Groundwater and surface water interactions at Georgetown Lake, Montana with emphasis on quantification of groundwater contribution. MSc Thesis, Montana Tech of the University of Montana, Butte, MT, 70.

Morgenstern, U., Daughney, C. J., Leonard, G., Gordon, D., Donath, F. M., & Reeves, R. (2015). Using groundwater age and hydrochemistry to understand sources and dynamics of nutrient contamination through the catchment into Lake Rotorua, New Zealand. *Hydrology and Earth System Sciences*, 19(2), 803–822. https://doi.org/10.5194/hess-19-803-2015

Morse, J. W., & Mackenzie, F. T. (1990). Geochemistry of sedimentary carbonates. In *Developments in sedimentology*. Elsevier.

Mukherjee, A., & Fryar, A. E. (2008). Deeper groundwater chemistry and geochemical modeling of the arsenic affected western Bengal basin, West Bengal, India. *Applied Geochemistry*, 23(4), 863–894. https://doi.org/10.1016/j.apgeochem.2007.07.011

Murgulet, D., Cook, M., & Murgulet, V. (2016). Groundwater mixing between different aquifer types in a complex structural setting discerned by elemental and stable isotope geochemistry. *Hydrological Processes*, 30(3), 410–423. https://doi.org/10.1002/hyp.10589

Murray J. 2018. Waulsortian limestone: Geology and hydrogeology. Groundwater Matters: Science and Practice Irish IAH National Meeting 2018, 10.

Musgrove, M., Stern, L. A., & Banner, J. L. (2010). Springwater geochemistry at Honey Creek state natural area, Central Texas: Implications for surface water and groundwater interaction in a karst aquifer. *Journal of Hydrology*, 388(1–2), 144–156. https://doi.org/10.1016/j.jhydrol.2010.04.036

Nyquist, J. E., Freyer, P. A., & Toran, L (2008). Stream bottom resistivity tomography to map ground water discharge. *Groundwater*, 46(4), 561–569.

O'Connell DW. 2015. Hydrogeochemistry and sources of water to a hypereutrophic groundwater fed lake (Lough Gur, Co Limerick). MSc, University of Birmingham.

O'Connell, D. W., Ansems, N., Kukkadapu, R. K., Jaisi, D., Orihel, D. M., Cade-Menun, B. J., Hu, Y., Wiklund, J., Hall, R. I., Chessell, H., Behrends, T., & Van Cappellen, P. (2020). Changes in sedimentary phosphorus burial following artificial eutrophication of Lake 227, Experimental Lakes area, Ontario, Canada. *Journal of Geophysical Research: Biogeosciences*, 125, e2020JG005713. https://doi.org/10.1029/2020JG005713

O'Connell, D. W., Mark Jensen, M., Jakobsen, R., Thamdrup, B., Joest Andersen, T., Kovacs, A., & Bruun Hansen, H. C. (2015). Vivianite formation and its role in phosphorus retention in Lake Ørn, Denmark. *Chemical Geology*, 409, 42–53. https://doi.org/10.1016/j.chemgeo.2015.05.002

Oliveira Ommen, D. A., Kidmose, J., Karan, S., Flindt, M. R., Engesgaard, P., Nilsson, B., & Andersen, F. O. (2012). Importance of groundwater and macrophytes for the nutrient balance at oligotrophic Lake Hampen, Denmark. *Ecohydrology*, 5(3), 286–296. https://doi.org/10.1002/eco.213

Panno, S. V., Hackley, K. C., Kelly, W. R., & Hwang, H.-H. (2006). Isotopic evidence of nitrate sources and denitrification in the Mississippi River, Illinois. *Journal of Environmental Quality*, 35(2), 495–504. https://doi.org/10.2134/jeq2005.0012

Perrin, A.-S., Probst, A., & Probst, J.-L. (2008a). Impact of nitrogenous fertilizers on carbonate dissolution in small agricultural catchments: Implications for weathering CO_2 uptake at regional and global scales. *Geochimica et Cosmochimica Acta*, 72(13), 3105–3123. https://doi.org/10.1016/j.gca.2008.04.011

Perrin, A.-S., Probst, A., & Probst, J.-L. (2008b). Impact of nitrogenous fertilizers on carbonate dissolution in small agricultural catchments: Implications for weathering CO_2 uptake at regional and global scales. *Geochimica et Cosmochimica Acta*, 72(13), 3105–3123. https://doi.org/10.1016/j.gca.2008.04.011

Petermann, E., Gibson, J. J., Knöller, K., Pannier, T., Weiß, H., & Schubert, M. (2018a). Determination of groundwater discharge rates and water residence time of groundwater-fed lakes by stable isotopes of water (18O, 2H) and radon (222Rn) mass balances. *Hydrological Processes*, 32(6), 805–816. https://doi.org/10.1002/hyp.11456

Petermann, E., Gibson, J. J., Knöller, K., Pannier, T., Weiß, H., & Schubert, M. (2018b). Determination of groundwater discharge rates and water residence time of groundwater-fed lakes by stable isotopes of water (18O, 2H) and radon (222Rn) mass balances. *Hydrological Processes*, 32(6), 805–816. https://doi.org/10.1002/hyp.11456

Qian, H., Wu, J., Zhou, Y., & Li, P. (2014). Stable oxygen and hydrogen isotopes as indicators of lake water recharge and evaporation in the lakes of the Yinchuan plain. *Hydrological Processes*, 28(10), 3554–3562. https://doi.org/10.1002/hyp.9915

Qin, D., Zhao, Z., Guo, Y., Liu, W., Haji, M., Wang, X., Xin, B., Li, Y., & Yang, Y. (2017a). Using hydrochemical, stable isotope, and river water recharge data to identify groundwater flow paths in a deeply buried karst system. *Hydrological Processes*, 31(24), 4297–4314. https://doi.org/10.1002/hyp.11356

Qin, D., Zhao, Z., Guo, Y., Liu, W., Haji, M., Wang, X., Xin, B., Li, Y., & Yang, Y. (2017b). Using hydrochemical, stable isotope, and river water recharge data to identify groundwater flow paths in a deeply buried karst system. *Hydrological Processes*, 31(24), 4297–4314. https://doi.org/10.1002/hyp.11356

Raymond, P. A., Hartmann, J., Lauerwald, R., Sobek, S., McDonald, C., Hoover, M., Butman, D., Striegl, R., Mayorga, E., Humborg, C., Kortelainen, P., Dürr, H., Meybeck, M., Ciais, P., & Guth, P. (2013). Global carbon dioxide emissions from inland waters. *Nature*, 503(7476), 355–359. https://doi.org/10.1038/nature12760

Rivett, M. O., Ellis, P. A., Greswell, R. B., Ward, R. S., Roche, R. S., Cleverly, M. G., Walker, C., Conran, D., Fitzgerald, P. J., Willcox, T., & Dowle, J. (2008). Cost-effective mini drive-point piezometers and multilevel samplers for monitoring the hyporheic zone. *Quarterly Journal of Engineering Geology and Hydrogeology*, 41(1), 49–60. https://doi.org/10.1144/1470-9236/07-012

Rocha, C., Veiga-Pires, C., Scholten, J., Knoeller, K., Gröcke, D. R., Carvalho, L., Anibal, J., & Wilson, J. (2016). Assessing land-ocean connectivity via submarine groundwater discharge (SGD) in the ria Formosa lagoon (Portugal): Combining radon measurements and stable isotope hydrology. *Hydrology and Earth System Sciences*, 20(8), 3077–3098. https://doi.org/10.5194/hess-20-3077-2016

Rudnick, S., Lewandowski, J., & Nützmann, G. (2015). Investigating groundwater-lake interactions by hydraulic heads and a water balance. *Groundwater*, 53(2), 227–237. https://doi.org/10.1111/gwat.12208

Rusjan, S., Sapač, K., Petrič, M., Lojen, S., & Bezak, N. (2019). Identifying the hydrological behavior of a complex karst system using stable isotopes. *Journal of Hydrology*, 577, 123956. https://doi.org/10.1016/j.jhydrol.2019.123956

Schallenberg, M., de Winton, M. D., Verburg, P., Kelly, D. J., Hamill, K. D., & Hamilton, D. P. (2013). Ecosystem services of lakes. In *Ecosystem Services in New Zealand – Conditions and trends*. Whenua Press.

Schwartz, F. W., & Zhang, H. (2003). *Fundamentals of ground water*. Wiley.

Shaw, G. D., Mitchell, K. L., & Gammons, C. H. (2017). Estimating groundwater inflow and leakage outflow for an intermontane lake with a structurally complex geology: Georgetown Lake in Montana, USA. *Hydrogeology Journal*, 25(1), 135–149. https://doi.org/10.1007/s10040-016-1500-1

Shaw, G. D., White, E. S., & Gammons, C. H. (2013). Characterizing groundwater-lake interactions and its impact on lake water quality. *Journal of Hydrology*, 492, 69–78. https://doi.org/10.1016/j.jhydrol.2013.04.018

Shin, W. J., Chung, G. S., Lee, D., & Lee, K. S. (2011). Dissolved inorganic carbon export from carbonate and silicate catchments estimated from carbonate chemistry and δ 13C DIC. *Hydrology and Earth System Sciences*, 15(8), 2551–2560. https://doi.org/10.5194/hess-15-2551-2011

Sironić, A., Barešić, J., Horvatinčić, N., Brozinčević, A., Vurnek, M., & Kapelj, S. (2017). Changes in the geochemical parameters of karst lakes over the past three decades – The case of Plitvice Lakes, Croatia. *Applied Geochemistry*, 78, 12–22. https://doi.org/10.1016/j.apgeochem.2016.11.013

Somerville, I. D., Strogen, P., & Jones, G. L. I. (1992). The biostratigraphy of Dinantian limestones and associated volcanic rocks in the Limerick syncline, Ireland. *Sedimentary Geology*, 79(1–4), 59–75.

Stoliker, D. L., Repert, D. A., Smith, R. L., Song, B., LeBlanc, D. R., McCobb, T. D., Conaway, C. H., Hyun, S. P., Koh, D.-C., Moon, H. S., & Kent, D. B. (2016). Hydrologic controls on nitrogen cycling processes and functional gene abundance in sediments of a groundwater flow-through Lake. *Environmental Science and Technology*, 50(7), 3649–3657. https://doi.org/10.1021/acs.est.5b06155

Stroj, A., Briški, M., & Oštrić, M. (2020). Study of groundwater flow properties in a karst system by coupled analysis of diverse environmental tracers and discharge dynamics. *Water (Switzerland)*, 12(9). https://doi.org/10.3390/w12092442

Stumm, W., & Morgan, J. (1981). *Aquatic chemistry*. Wiley.

Szramek, K., McIntosh, J. C., Williams, E. L., Kanduc, T., Ogrinc, N., & Walter, L. M. (2007). Relative weathering intensity of calcite versus dolomite in carbonate-bearing temperate zone watersheds: Carbonate geochemistry and fluxes from catchments within the St. Lawrence and Danube river basins. *Geochemistry, Geophysics, Geosystems*, 8(4), Q04002. https://doi.org/10.1029/2006GC001337

Tondu, J. M. E., Turner, K. W., Wolfe, B. B., Hall, R. I., Edwards, T. W. D., & McDonald, I. (2013). Using water isotope tracers to develop the hydrological component of a long-term aquatic ecosystem monitoring program for a northern lake-rich landscape. *Arctic, Antarctic, and Alpine Research*, 45(4), 594–614. https://doi.org/10.1657/1938-4246-45.4.594

Wilson, J., Coxon, C., & Rocha, C. (2016). A GIS and remote sensing based screening tool for assessing the potential for groundwater discharge to lakes in Ireland. *Biology and Environment*, 116B(3), 265. https://doi.org/10.3318/BIOE.2016.15

Wilson, J., & Rocha, C. (2012). Regional scale assessment of submarine groundwater discharge in Ireland combining medium resolution satellite imagery and geochemical tracing techniques. *Remote Sensing of Environment*, 119, 21–34. https://doi.org/10.1016/j.rse.2011.11.018

Wilson, J., & Rocha, C. (2016). A combined remote sensing and multitracer approach for localisingand assessing groundwater-lake interactions. *International Journal of Applied Earth Observation and Geoinformation*, 44, 195–204.

Xiao, J., Jin, Z. D., Wang, J., & Zhang, F. (2015). Hydrochemical characteristics, controlling factors and solute sources of groundwater within the Tarim River basin in the extreme arid region, NW Tibetan plateau. *Quaternary International*, 380–381, 237–246. https://doi.org/10.1016/j.quaint.2015.01.021

Yang, Q., Xiao, H., Zhao, L., Yang, Y., Li, C., Zhao, L., & Yin, L. (2011). Hydrological and isotopic characterization of river water, groundwater, and groundwater recharge in the Heihe River basin, northwestern China. *Hydrological Processes*, 25(8), 1271–1283. https://doi.org/10.1002/hyp.7896

Yin, C., Yang, H., Wang, J., Guo, J., Tang, X., & Chen, J. (2020). Combined use of stable nitrogen and oxygen isotopes to constrain the nitrate sources in a karst lake. *Agriculture, Ecosystems and Environment*, 303, 107089. https://doi.org/10.1016/j.agee.2020.107089

Yu, S., Chae, G., Oh, J., Kim, S.-H., Kim, D.-I., & Yun, S.-T. (2021). Hydrochemical and isotopic difference of spring water depending on flow

type in a stratigraphically complex karst area of South Korea. *Frontiers in Earth Science*, 9, 712865. https://doi.org/10.3389/feart.2021.712865

Yue, F.-J., Li, S.-L., Liu, C.-Q., Lang, Y.-C., & Ding, H. (2015a). Sources and transport of nitrate constrained by the isotopic technique in a karst catchment: An example from Southwest China. *Hydrological Processes*, 29(8), 1883–1893. https://doi.org/10.1002/hyp.10302

Yue, F.-J., Li, S.-L., Liu, C.-Q., Lang, Y.-C., & Ding, H. (2015b). Sources and transport of nitrate constrained by the isotopic technique in a karst catchment: An example from Southwest China. *Hydrological Processes*, 29(8), 1883–1893. https://doi.org/10.1002/hyp.10302

Zhan, L., Chen, J., Zhang, S., Li, L., Huang, D., & Wang, T. (2016). Isotopic signatures of precipitation, surface water, and groundwater interactions, Poyang Lake Basin, China. *Environmental Earth Sciences*, 75(19), 712865. https://doi.org/10.1007/s12665-016-6081-8

Zhang, B., Zhao, D., Zhou, P., Qu, S., Liao, F., & Wang, G. (2020). Hydrochemical characteristics of groundwater and dominant water–rock interactions in the Delingha area, Qaidam Basin, Northwest China. *Water*, 12(3), 836. https://doi.org/10.3390/w12030836

Zhao, M., Liu, Z., Li, H.-C., Zeng, C., Yang, R., Chen, B., & Yan, H. (2015). Response of dissolved inorganic carbon (DIC) and δ13CDIC to changes in climate and land cover in SW China karst catchments. *Geochimica et Cosmochimica Acta*, 165, 123–136. https://doi.org/10.1016/j.gca.2015.05.041

Zhou, P., Li, M., & Lu, Y. (2017). Hydrochemistry and isotope hydrology for groundwater sustainability of the coastal multilayered aquifer system (Zhanjiang, China). *Geofluids*, 2017, 1–19. https://doi.org/10.1155/2017/7080346

Zhu, B., Yang, X., Rioual, P., Qin, X., Liu, Z., Xiong, H., & Yu, J. (2011). Hydrogeochemistry of three watersheds (the Erlqis, Zhungarer and Yili) in northern Xinjiang, NW China. *Applied Geochemistry*, 26(8), 1535–1548. https://doi.org/10.1016/j.apgeochem.2011.06.018

SUPPORTING INFORMATION

Additional supporting information can be found online in the Supporting Information section at the end of this article.